

IN THE UNITED STATES PATENT AND TRADEMARK OFFICE

BEFORE THE PATENT TRIAL AND APPEAL BOARD

MIM SOFTWARE INC.
Petitioner

v.

EXINI Diagnostics AB.
Patent Owner

U.S. PATENT NO. 11,941,817
Filing Date: March 29, 2023
Issue Date: March 26, 2024
Title: SYSTEMS AND METHODS FOR PLATFORM AGNOSTIC WHOLE
BODY IMAGE SEGMENTATION

Inter Partes Review No.: IPR2025-00827

**PETITION FOR *INTER PARTES* REVIEW OF
U.S. PATENT NO. 11,941,817**

Mail Stop: Patent Board
Patent Trial and Appeal Board
U.S. Patent and Trademark Office
P.O. Box 1450
Alexandria, VA 22313-1450

TABLE OF CONTENTS

I.	MANDATORY NOTICES (37 C.F.R. §42.8(A)(1))	1
A.	Real Party-in-Interest (37 C.F.R. §42.8(b)(1)).....	1
B.	Related Matters (37 C.F.R. §42.8(b)(2)).....	1
C.	Lead and Back-up Counsel and Service Information (37 C.F.R. §42.8(b)(3)-(4)).....	2
II.	INTRODUCTION AND RELIEF REQUESTED.....	2
III.	FOUNDATIONS FOR STANDING AND FEES	5
IV.	THE PATENT AND PROSECUTION HISTORY	5
A.	Specification	5
B.	Prosecution History	7
V.	IDENTIFICATION OF CHALLENGE.....	8
VI.	LEVEL OF SKILL IN THE ART.....	8
VII.	CLAIM CONSTRUCTION (37 C.F.R. §42.100(b)).....	9
A.	3D Segmentation Map (Claims 1, 3, 10, 12, 19, 26).....	9
VIII.	DETAILED EXPLANATION OF INVALIDITY GROUNDS.....	10
A.	Summary of the Prior Art	10
1.	US2012/0123253 (“Renisch”)	10
2.	US10,140,544 (“Zhao”)	12
3.	US2018/0144828 (“Baker”).....	13
4.	The PROMISE Criteria (“Eiber”).....	15
5.	US2011/0007954 (“Suehling”).....	16
B.	Grounds A and B: Anticipation by Renisch or Obviousness over Renisch in view of Zhao.....	18
1.	Claim 1: Method Claim.....	18
2.	Claim 2: “The method of claim 1, comprising using, by the processor, the one or more detected hotspots to determine a cancer status for the subject.”	31
3.	Claim 3	32

4. Claim 4: “The method of claim 3, wherein the reference tissue regions comprise one or more members selected from the group consisting of: a liver, an aorta, and a parotid gland.”	36
5. Claim 5: “The method of claim 2, comprising, determining, by the processor, an overall index value indicative of a cancer status of the subject using at least a portion of the one or more hotspot index values.”	36
6. Claim 7: “The method of claim 1, wherein: the 3D anatomical image is an x-ray computed tomography (CT) image, and the 3D functional image is a 3D positron emission tomography (PET) image.”	37
7. Claim 19	38
8. Claims 10-14, 16, and 26: System Claims	41
C. Ground C and D, Obviousness over Renisch, or Renisch-Zhao, each in view of Baker or Eiber	43
1. Claim 8/17: “The [method/system] of claim [7/16], wherein the 3D PET image of the subject is obtained following administration to the subject of a radiopharmaceutical comprising a prostate-specific membrane antigen (PSMA) binding agent.”	43
2. Claims 9/18: “The [method/system] of claim [8/17], wherein the radiopharmaceutical comprises [¹⁸ F]DCFPyL.”	46
3. Claim 22/29: “The [method/system] of claim [8/17], wherein the radiopharmaceutical comprises ⁶⁸ Ga-PSMA-11.”	46
4. Claims 23/30: “The method of claim [8/17], wherein the radiopharmaceutical comprises ⁶⁸ Ga-PSMA-617.”	47
5. Claims 24/31: “The method of claim [8/17], wherein the radiopharmaceutical comprises ⁶⁸ Ga-PSMA-I&T.”	47
6. Claims 25/32: “The method of claim [8/17], wherein the radiopharmaceutical comprises ¹⁸ F-PSMA-1007.”	47
D. Ground E, Obviousness Over Baker in view of Zhao	48
1. Claim 1	48
2. Claim 2: Using hotspots to determine cancer status	54
3. Claim 7: Computed tomography (CT) and positron emission tomography (PET) images	55
4. Claim 8: PET image obtained following administration of PSMA	56
5. Claims 9 and 22-25: Specific radiopharmaceuticals	56

6. Claims 10-11, 16-18, and 29-32	56
E. Ground F, Obviousness over Baker-Zhao in view of Eiber.....	57
1. Claim 3/12.....	57
2. Claims 4/13: Reference tissue regions selected from liver, aorta, and parotid gland	62
3. Claims 5/14: Overall index value indicative of cancer status.....	62
F. Ground G, Obviousness over Baker-Zhao in view of Suehling.....	63
1. Claims 19/26	63
2. Claim 28: “The system of claim 26, wherein the particular target tissue region is selected from the group consisting of: a skeletal region comprising one or more bones of the subject, a lymph region, and a prostate region.”	69
IX. INSTITUTION IS APPROPRIATE	70
X. CONCLUSION	71

EXHIBIT LIST

No.	Description
Ex1001	U.S. Patent No. 11,941,817 (“the Patent”)
Ex1002	Declaration of Dr. Bruce Rosen
Ex1003	Dr. Rosen Curriculum Vitae
Ex1004	Prosecution History File of the Patent (Application No. 18/127,991)
Ex1005	U.S. Patent Application Publication No. 2012/0123253 (“Renisch”)
Ex1006	U.S. Patent Application Publication No. 2011/0007954 (“Suehling”)
Ex1007	U.S. Patent No. 10,140,544 (“Zhao”)
Ex1008	U.S. Patent Application Publication No. 2018/0144828 (“Baker”)
Ex1009	Eiber, “Prostate Cancer Molecular Imaging Standardized Evaluation (PROMISE): Proposed miTNM Classification for the Interpretation of PSMA-Ligand PET/CT,” <i>The Journal of Nuclear Medicine</i> 59(3):469-478 (March 2018) (“Eiber”)
Ex1010	U.S. Patent Application Publication No. 2010/0032575 (“Iagaru”)
Ex1011	U.S. Patent Application Publication No. 2015/0287188 (“Gazit”)
Ex1012	RESERVED
Ex1013	Second Amended Complaint, <i>Progenics Pharmaceuticals, Inc. v. MIM Software Inc.</i> , Case No. 1:24-cv-10437-PBS, Dkt. 25, April 5, 2024.
Ex1014	U.S. Patent No. 8,855,387 (“Hamadeh”)
Ex1015	Kaur, “Various Image Segmentation Techniques: A Review,” <i>International Journal of Computer Science and Mobile Computing</i> 3(5):809-814 (May 5, 2014) (“Kaur”)
Ex1016	Sharma, “Automated medical image segmentation techniques,” <i>Journal of Medical Physics</i> 35(1):3-14 (2010) (“Sharma”)
Ex1017	Greenspan, “Deep Learning in Medical Imaging: Overview and Future Promise of an Exciting New Technique,” <i>IEEE Transactions on Medical Imaging</i> 35(5):1153-1159 (May 2016) (“Greenspan”)
Ex1018	Litjens, “A Survey on Deep Learning in Medical Image Analysis,” <i>Medical Image Analysis</i> 42:60-88 (Dec. 2017) (“Litjens”)
Ex1019	Shen, “Deep Learning in Medical Image Analysis,” <i>Annual Review of Biomedical Engineering</i> 19:221-248 (2017) (“Shen”)
Ex1020	Gandaglia, “Distribution of metastatic sites in patients with

prostate cancer: A population-based analysis,” <i>The Prostate</i> 74(2):210-216 (2014) (“Gandaglia”)
--

CLAIMS APPENDIX

Limitation	Claim Language
Claim 1	
[1(pre)]	A method for automatically processing 3D images to automatically identify cancerous lesions within a subject, the method comprising:
[1(a)]	(a) receiving, by a processor of a computing device, a 3D anatomical image of a subject obtained using an anatomical imaging modality, wherein the 3D anatomical image comprises a graphical representation of tissue within the subject;
[1(b)]	(b) automatically identifying, by the processor, using one or more machine learning modules, for each of a plurality of target tissue regions, a corresponding target volume of interest (VOI) within the 3D anatomical image;
[1(c)]	(c) determining, by the processor, a 3D segmentation map representing a plurality of 3D segmentation masks, each 3D segmentation mask representing a particular identified target VOI;
[1(d)]	(d) receiving, by the processor, a 3D functional image of the subject obtained using a functional imaging modality;
[1(e)]	(e) identifying, within the 3D functional image, one or more 3D volume(s), each corresponding to an identified target VOI, using the 3D segmentation map; and
[1(f)]	(f) automatically detecting, by the processor, within at least a portion of the one or more 3D volumes identified within the 3D functional image, one or more hotspots determined to represent lesions based on intensities of voxels within the 3D functional image.
Claim 2	
[2]	The method of claim 1, comprising using, by the processor, the one or more detected hotspots to determine a cancer status for the subject.
Claim 3	
[3(pre)]	The method of claim 1, wherein the target tissue regions comprise one or more reference tissue regions and wherein the method comprises:
[3(a)]	using the 3D segmentation map to identify, by the processor, within the 3D functional image, one or more 3D reference volume(s), each corresponding to a particular reference tissue region;
[3(b)]	determining, by the processor, one or more reference intensity values, each associated with a particular 3D reference volume of the

	one or more 3D reference volume(s) and corresponding to a measure of intensity within the particular 3D reference volume;
[3(c)]	determining, by the processor, one or more individual hotspot intensity values, each associated with a particular hotspot of at least a portion of the detected one or more hotspots and corresponding to a measure of intensity of the particular hotspot; and
[3(d)]	determining, by the processor, one or more individual hotspot index values using the one or more individual hotspot intensity values and the one or more reference intensity values.
Claim 4	
[4]	The method of claim 3, wherein the reference tissue regions comprise one or more members selected from the group consisting of: a liver, an aorta, and a parotid gland.
Claim 5	
[5]	The method of claim 2, comprising, determining, by the processor, an overall index value indicative of a cancer status of the subject using at least a portion of the one or more hotspot index values.
Claim 7	
[7]	The method of claim 1, wherein: the 3D anatomical image is an x-ray computed tomography (CT) image, and the 3D functional image is a 3D positron emission tomography (PET) image.
Claim 8	
[8]	The method of claim 7, wherein the 3D PET image of the subject is obtained following administration to the subject of a radiopharmaceutical comprising a prostate-specific membrane antigen (PSMA) binding agent.
Claim 9	
[9]	The method of claim 8, wherein the radiopharmaceutical comprises [¹⁸ F]DCFPyL.
Claim 10	
[10(pre)]	A system for automatically processing 3D images to automatically identify cancerous lesions within a subject, the system comprising:
[10(i)]	a processor of a computing device; and a memory having instructions stored thereon, wherein the instructions, when executed by the processor, cause the processor to:
[10(ii)]	(a) receive a 3D anatomical image of a subject obtained using an

	anatomical imaging modality, wherein the 3D anatomical image comprises a graphical representation of tissue within the subject;
[10(iii)]	(b) automatically identify, using one or more machine learning modules, for each of a plurality of target tissue regions, a corresponding target volume of interest (VOI) within the 3D anatomical image;
[10(iv)]	(c) determine a 3D segmentation map representing a plurality of 3D segmentation masks, each 3D segmentation mask representing a particular identified target VOI;
[10(v)]	(d) receive a 3D functional image of the subject obtained using a functional imaging modality;
[10(vi)]	(e) identify, within the 3D functional image, one or more 3D volume(s), each corresponding to an identified target VOI, using the 3D segmentation map; and
[10(vii)]	(f) automatically detect, within at least a portion of the one or more 3D volumes identified within the 3D functional image, one or more hotspots determined to represent lesions based on intensities of voxels within the 3D functional image.
Claim 11	
[11]	The system of claim 10, wherein the instructions cause the processor to use the one or more detected hotspots to determine a cancer status for the subject.
Claim 12	
[12(pre)]	The system of claim 10, wherein the target tissue regions comprise one or more reference tissue regions and wherein the instructions cause the processor to:
[12(a)]	use the 3D segmentation map to identify, within the 3D functional image, one or more 3D reference volume(s), each corresponding to a particular reference tissue region;
[12(b)]	determine one or more reference intensity values, each associated with a particular 3D reference volume of the one or more 3D reference volume(s) and corresponding to a measure of intensity within the particular 3D reference volume;
[12(c)]	determine one or more individual hotspot intensity values, each associated with a particular hotspot of at least a portion of the detected one or more hotspots and corresponding to a measure of intensity of the particular hotspot; and
[12(d)]	determine one or more individual hotspot index values using the one or more individual hotspot intensity values and the one or more

	reference intensity values.
Claim 13	
[13]	The system of claim 12, wherein the reference tissue regions comprise one or more members selected from the group consisting of: a liver, an aorta, and a parotid gland.
Claim 14	
[14]	The system of claim 11, wherein the instructions cause the processor to determine an overall index value indicative of a cancer status of the subject using at least a portion of the one or more hotspot index values.
Claim 16	
[16]	The system of claim 10, wherein: the 3D anatomical image is an x-ray computed tomography (CT) image, and the 3D functional image is a 3D positron emission tomography (PET) image.
Claim 17	
[17]	The system of claim 16, wherein the 3D PET image of the subject is obtained following administration to the subject of a radiopharmaceutical comprising a prostate-specific membrane antigen (PSMA) binding agent.
Claim 18	
[18]	The system of claim 17, wherein the radiopharmaceutical comprises [¹⁸ F]DCFPyL.
Claim 19	
[19(pre)]	The method of claim 1, wherein the nuclear medicine image is a SPECT scan.
[19(a)]	at step (e), using the 3D segmentation map to identify, within the 3D functional image, as at least a portion of the one or more 3D volumes, one or more 3D background tissue volume(s), each corresponding a particular background tissue region; and
[19(b)]	excluding voxels of the 3D within the 3D background tissue from the voxels used to automatically detect the one or more hotspots at step (f).
Claim 22	
[22]	The method of claim 8, wherein the radiopharmaceutical comprises ⁶⁸ Ga-PSMA-11.
Claim 23	
[23]	The method of claim 8, wherein the radiopharmaceutical

	comprises ⁶⁸ Ga-PSMA-617.
Claim 24	
[24]	The method of claim 8, wherein the radiopharmaceutical comprises ⁶⁸ Ga-PSMA-I&T.
Claim 25	
[25]	The method of claim 8, wherein the radiopharmaceutical comprises ¹⁸ F-PSMA-1007.
Claim 26	
[26(pre)]	The system of claim 10, wherein the target tissue regions comprise one or more background tissue regions and wherein the instructions cause the processor to:
[26(a)]	at step (e), using the 3D segmentation map to identify, within the 3D functional image, as at least a portion of the one or more 3D volumes, one or more 3D background tissue volume(s), each corresponding a particular background tissue region; and
[26(b)]	exclude voxels of the 3D within the 3D background tissue from the voxels used to automatically detect the one or more hotspots at step (f).
Claim 28	
[28]	The claim of 26, wherein the particular target tissue region is selected from the group consisting of: a skeletal region comprising one or more bones of the subject, a lymph region, and a prostate region.
Claim 29	
[29]	The system of claim 17, wherein the radiopharmaceutical comprises ⁶⁸ Ga-PSMA-11.
Claim 30	
[30]	The method of claim 17, wherein the radiopharmaceutical comprises ⁶⁸ Ga-PSMA-617.
Claim 31	
[31]	The method of claim 17, wherein the radiopharmaceutical comprises ⁶⁸ Ga-PSMA-I&T.
Claim 32	
[32]	The method of claim 17, wherein the radiopharmaceutical comprises ¹⁸ F-PSMA-1007.

I. MANDATORY NOTICES (37 C.F.R. §42.8(A)(1))

A. Real Party-in-Interest (37 C.F.R. §42.8(b)(1))

The real parties-in-interest are Petitioner MIM Software Inc. (“Petitioner”); Petitioner’s parent company, GE HealthCare Technologies Inc.; and Petitioner’s insurer, AIG Specialty Insurance Company.

B. Related Matters (37 C.F.R. §42.8(b)(2))

EXINI Diagnostics AB (“EXINI” or “Patent Owner”) has asserted U.S. Patent No. 11,941,817 (“the Patent”) against Petitioner in *Progenics Pharmaceuticals, Inc. et al v. MIM Software Inc.*, 1:24-cv-10437-PBS (D. Mass.) (“MA Litigation”). Ex1013. The earliest date of service is April 5, 2024.

Additional patents asserted against Petitioner in the MA Litigation include U.S. Patent Nos. 10,665,346; 11,424,035; and 11,894,141. These three patents contain subject matter that overlaps with the subject matter described in the Patent. They are not, however, within the same patent family as the Patent and are not related to the Patent by any priority claim. Petitioner has filed a Petition for *Inter Partes* Review of U.S. Patent No. 10,665,346 in IPR2025-00630. Petitioner has filed a Petition for *Inter Partes* Review of U.S. Patent No. 11,424,035 in IPR2025-00725. Petitioner has filed a Petition for *Inter Partes* Review of U.S. Patent No. 11,894,141 in IPR2025-00726.

C. Lead and Back-up Counsel and Service Information (37 C.F.R. §42.8(b)(3)-(4))

Lead counsel is Jeff Metzcar (No. 52,027) at THOMPSON HINE LLP, 10050 Innovation Drive, Suite 400, Dayton, OH 45342; Jeff.Metzcar@thompsonhine.com. Backup counsel is David R. Jaglowski (No. 58,514) at THOMPSON HINE LLP, 41 South High Street, Suite 1700, Columbus, Ohio 43215; David.Jaglowski@thompsonhine.com. Supplemental backup counsel is Marla R. Butler (to be admitted *pro hac vice*) at THOMPSON HINE LLP, Two Alliance Center, 3560 Lenox Road Suite 1600, Atlanta, Georgia 30326; Marla.Butler@thompsonhine.com. Petitioner consents to email service at the following address: IPDocket@ThompsonHine.com.

II. INTRODUCTION AND RELIEF REQUESTED

Petitioner requests *inter partes* review (IPR) and a finding that claims 1-5, 7-14, 16-19, 22-26, and 28-32 (the “challenged claims”) of U.S. Patent No. 11,941,817 (“the Patent,” Ex1001) are not patentable.

The Patent claims systems and methods for “automatically processing 3D images to automatically identify cancerous lesions within a subject.” *See, e.g.*,

Ex1001, claims 1, 10¹. More specifically, the Patent claims systems and methods that use “machine learning” to automatically identify one or more “target volume of interest (VOI) within [a] 3D anatomical image” (e.g., CT or MRI), which is then mapped to a “3D functional image” (e.g., PET or SPECT) to “identify[], within the 3D functional image, one or more 3D volume(s), each corresponding to an identified target VOI.” *Id.*

The specific application to 3D images is emphasized, not only in the Patent’s claims, but also in the written description, which opens the “Summary of the Invention” by stating: “Presented herein are systems and methods that provide for automated analysis of three-dimensional (3D) medical images of a subject in order to automatically identify specific 3D volumes within the 3D images that correspond to specific anatomical regions, e.g., organs and/or tissue.” Ex1001, 3:1-7. Indeed, the Patent touts that “[t]he capability of the approaches described herein to handle 3D images is an important advantage over certain other image analysis that only identify 2D regions in 2D images.” Ex1001, 3:21-24. With specific reference to – “see also” – the Patent Owner’s prior “U.S. Pat. No. 8,855,387, issued Oct. 7, 2014,” the Patent states that “one approach relevant for cancer

¹ Unless otherwise indicated, all emphasis, ellipses, and bracketed language has been added in the quotations and citations presented herein.

detection [is] EXINI Diagnostics AB's Bone Scan Index (BSI)" but "the BSI analysis is carried out on two-dimensional scintigraphy images, as opposed to on three dimensional images." Ex1001, 3:24-29.

The Patent was apparently not rigorously compared against the most pertinent prior art during Examination – especially art that automatically identifies cancerous lesions in 3D medical images. The Examiner allowed all claims, without any rejection, stating in his Reasons for Allowance, that the "**closest prior art**" is US 8,855,387 ("Hamadeh") (Ex1014), *i.e.*, the very same patent that was distinguished from the purported invention because it is limited to 2D images. Ex1004, pp.323 (emphasis in original). Not only does Hamadeh not analyze 3D medical images, as claimed, it does not even segment anatomical images using machine learning as claimed. Ex1002, ¶¶ 65, 73; Ex1014, 1:16-20. Plainly, Hamadeh was not the closest available prior art, yet the Examiner did not substantively address, or even mention, any other prior art reference throughout the written record.

This Petition presents two alternative primary references, US2012/0123253 ("Renisch") and US2018/0144828 ("Baker"), both of which – unlike Hamadeh – automatically identify cancerous lesions in 3D medical images by: (i) segmenting 3D anatomical images using machine learning; and (ii) mapping the segmented regions, e.g., organs, to a corresponding 3D functional image to identify the

anatomical locations of lesions detected in the functional image. Although Renisch and Baker were disclosed to the Patent Office, they were not substantively addressed in the Patent's prosecution history, either alone or in the combinations presented in this Petition.

As detailed in this Petition and supporting Declaration from Dr. Rosen (Ex1002), the challenged claims of the Patent are unpatentable as anticipated and/or obvious in view of the presented prior art.

III. GROUNDS FOR STANDING AND FEES

Petitioner certifies that the Patent is available for *inter partes* review and Petitioner is not barred or estopped from requesting review.

The undersigned authorizes the charge of any required fees to Deposit Account No. 20-0809.

IV. THE PATENT AND PROSECUTION HISTORY

A. Specification

The Patent explains that “nuclear medicine cameras, known as single-photon emission computerized tomography (SPECT) or positron emission tomography (PET) cameras” can obtain *functional images* showing “the presence and the extent of disease in a patient.” Ex1001, 1:42-47. Other imaging modalities, such as computed tomography (CT) and magnetic resonance imaging (MRI), provide detailed anatomical information. Ex1001, 3:39-40. The Patent further explains that “[f]unctional images such as SPECT and PET provide detailed and specific

information on biological processes in the body, but their potential is only realized when combined with a detailed anatomical map so that function can be localized to individual organs and structures.” Ex1001, 3:34-39. Accordingly, the Patent proposes systems and methods to automatically segment a 3D anatomical image into specific tissue regions (Ex1001, 5:12-27, 10:45-12:16) and map the segmented tissue regions from the anatomical image to a corresponding 3D functional image (Ex1001, 32:65-33:8, 37:15-48). *See* Ex1001, 3:49-4:3.

The Patent states that each region segmented from an anatomical image may be represented by a “segmentation mask,” and “[t]he multiple segmentation masks, identifying multiple target tissue regions across a patient's body, can be stitched together to form a segmentation map.” Ex1001, 32:3-13. To locate corresponding regions in a functional image, “the individual segmentation masks (of the segmentation map) are mapped from the 3D anatomical image to the 3D functional image.” Ex1001, 37:15-22.

To detect cancerous lesions, the Patent explains that localized regions of high intensity within functional images, *i.e.*, hotspots, can be classified as cancerous or not by comparing the voxel intensities within the hotspot to one or more threshold values, including a region-specific (*i.e.*, organ-specific) threshold value. Ex1001, 8:3-10, 40:25-34, 41:27-34.

This entire process described above is generally summarized in Fig. 5B of

the Patent, which is reproduced below.

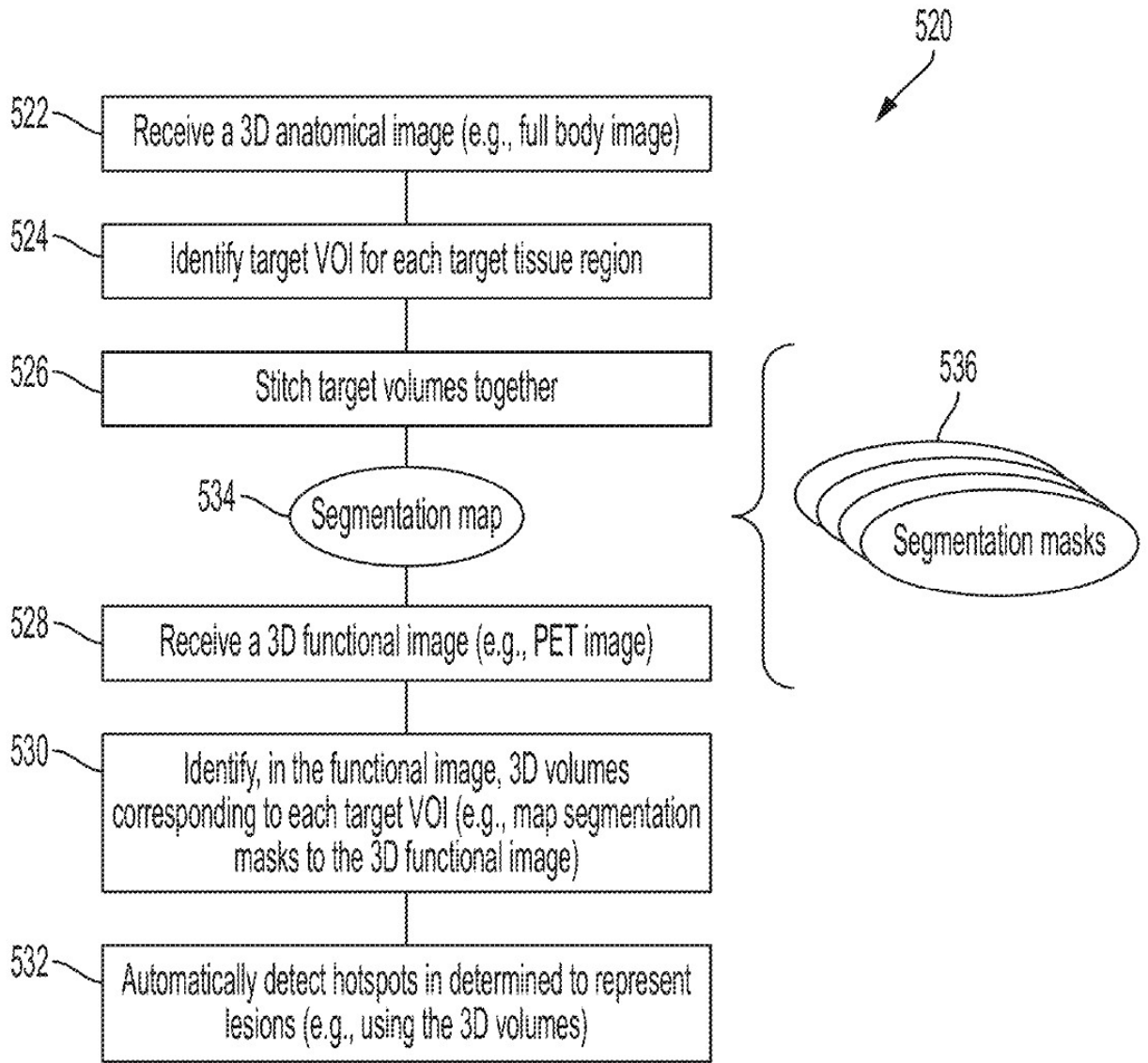


FIG. 5B

B. Prosecution History

The Patent was filed on March 29, 2023, as a division claiming earliest priority to provisional application no. 62/789,155, filed Jan. 7, 2019. Ex1001. By

October 13, 2023, the Examiner – without having made any claim rejections – issued a first Notice of Allowance, allowing all pending claims and stating: “**The closest prior art** is [EXINI’s] **Hamadeh et al. (US 8,855,387)**.” Ex1004, p.323 (emphasis in original). On November 21, 2023, the Examiner issued a second Notice of Allowance providing the same reasons for allowance. Ex1004, pp.421-431.

V. IDENTIFICATION OF CHALLENGE

Petitioner requests review of challenged claims 1-5, 7-14, 16-19, 22-26, and 28-32 of the Patent as follows:

Ground	Prior Art	Basis	Claims Challenged
A	Renisch	§102	1-5, 7, 10-14, 16, 19, 26
B	Renisch in view of Zhao (“Renisch-Zhao”)	§103	1-5, 7, 10-14, 16, 19, 26
C	Renisch, or Renisch-Zhao, each in view of Baker	§103	8-9, 17-18, 22-25, 29-32
D	Renisch, or Renisch-Zhao, each in view of Eiber	§103	8-9, 17-18, 22, 24-25, 29, 31-32
E	Baker in view of Zhao (“Baker-Zhao”)	§103	1-2, 7-11, 16-18, 22-25, 29-32
F	Baker-Zhao in view of Eiber	§103	3-5, 12-14
G	Baker-Zhao in view of Suehling	§103	19, 26, 28

VI. LEVEL OF SKILL IN THE ART

The hypothetical person of ordinary skill in the art (“POSITA”) would include a person with a medical (MD) degree and/or an advanced degree in

Computer Engineering, Computer Science, Physics, or other field related to computer imaging, and at least 3 years of field experience with medical imaging devices, such as PET/CT or SPECT/CT systems. Ex1002, ¶39.

VII. CLAIM CONSTRUCTION (37 C.F.R. §42.100(b))

Except for the term “3D segmentation map” the claim terms of the Patent do not require an express construction. Ex1002, ¶¶106-110.

A. 3D Segmentation Map (Claims 1, 3, 10, 12, 19, 26)

The Patent claims internally define a 3D segmentation map as “representing a plurality of 3D segmentation masks, each 3D segmentation mask representing a particular identified target VOI.” Ex1001, 79:19-22, 80:27-30. This description is consistent with the Patent specification, which explains that each 3D VOI corresponding to a specific target tissue region, such as an organ, may be represented via a segmentation mask, and “[t]he multiple segmentation masks, identifying multiple target tissue regions across a patient’s body, can be stitched together to form a segmentation map.” Ex1001, 32:6-13. Accordingly, for the purpose of this Petition, the term “3D segmentation map” can be construed simply as: “a plurality of 3D segmentation masks distinguishing a plurality of regions

within a 3D image.”² See Ex1002, ¶¶108-110.

VIII. DETAILED EXPLANATION OF INVALIDITY GROUNDS

A. Summary of the Prior Art

1. US2012/0123253 (“Renisch”)

Renisch is a United States patent application that published on May 17, 2012. Ex1005. It is prior art under 35 U.S.C. §102(a)(1) and (a)(2).

Renisch discloses a lesion identification system that automatically processes 3D anatomical and functional images of a patient to detect hotspots while suppressing from the detection results regions where normal physiological uptake of a radiotracer is expected, such as the brain or liver. Ex1005, [0006], [0020]-[0022]. Referring to Fig. 5 below, Renisch: (i) automatically segments 3D anatomical images (*e.g.*, CT or MR images) into volumes corresponding to anatomical structures (Ex1005, [0025]); (ii) automatically detects hotspots in corresponding 3D functional images (*e.g.*, PET or SPECT) based on voxel intensity (Ex1005, [0029]); (iii) suppresses detected hotspots determined to be

² Patent Owner has asserted that Petitioner infringes claim 1 of the Patent and that Petitioner’s accused product satisfies the limitation “determining, by the processor, a 3D segmentation map representing a plurality of 3D segmentation masks ...” merely “because ... [the accused product’s] physiological uptake removal technique involves creating 3D organ contours that represent and delineate particular organs, for example, in order to transfer them to 3D nuclear medicine (e.g., SPECT and/or PET) images.” Ex1013, ¶114.

normal physiological uptake based on their location relative to segmented organs (Ex1005, [0031]); and (iv) identifies unsuppressed hotspots as potential cancerous lesions or not (Ex1005, [0032]).

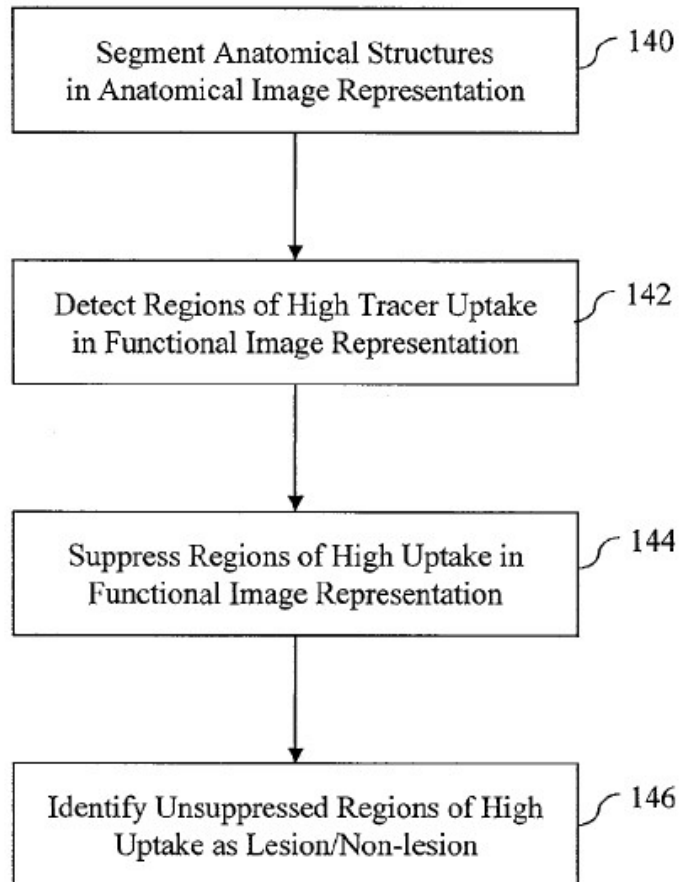


Figure 5

Renisch teaches that “[s]egmentation can ... be helpful for accurately determining a location of the hot spots relative to the patient’s anatomy” (Ex1005,

[0025]) and states that “anatomical regions identified in the anatomical first image representation can be carried over to the functional second image representation in order to delineate anatomical structures in the second image representation” (Ex1005, [0034] (reference numbers omitted)). Renisch also states that segmentation of organ structures in 3D anatomical images can be model-based, using “three-dimensional anatomical structure models,” or can be accomplished using machine learning algorithms such as clustering or artificial neural networks. Ex1005, [0025], [0027].

2. US10,140,544 (“Zhao”)

Zhao is a U.S. patent issued on November 27, 2018. Ex1007. It is prior art under 35 U.S.C. §102(a)(1) and (a)(2).

Zhao generally relates to digital “image segmentation,” which Zhao describes as the identification of regions-of-interest (ROIs) in digital images. Ex1007, Abstract, 5:11-23. Zhao teaches: “ROIs, once determined, may be represented by a digital mask containing a same number of pixels as the digital image or down-sized number of pixels from the digital image.” Ex1007, 5:25-28. “A digital mask may be alternatively referred to as a mask or segmentation mask.” Ex1007, 5:28-29. Zhao explains:

Each pixel of the mask may contain a value used to denote whether a particular corresponding pixel of the digital image is among any ROI, and if it is, which type of ROI among multiple types of ROIs does it

fall. For example, if there is only a single type of ROI, a binary mask is sufficient to represent all ROIs. In particular, each pixel of the ROI mask may be either zero or one, representing whether the pixel is or is not among the ROIs. For a mask capable of representing multiple types of ROI, each pixel may be at one of a number of values each corresponding to one type of ROIs. A multi-value mask, however, may be decomposed into a combination [sic] the more fundamental binary masks each for one type of ROI.

Ex1007, 5:30-42.

3. US2018/0144828 (“Baker”)

Baker is a U.S. patent application published on May 24, 2018. Ex1008. It is prior art under 35 U.S.C. §102(a)(1) and (a)(2).

Almost identically to the Patent, Baker discloses a system that automatically analyzes a patient’s 3D anatomical (e.g., CT) and 3D functional (e.g. PET or SPECT) images to detect areas of cancer and compute risk indices based on the level of cancerous tissue detected within one or more tissue regions (e.g., the skeleton). Ex1008, [0014], [0019]-[0020], [0136]-[0140].

Baker teaches that:

CT scans provide accurate anatomical information in the form of detailed three-dimensional (3D) images of internal organs, bones, soft tissue, and blood vessels. Accordingly, 3D boundaries of specific regions of imaged tissue can be accurately identified by analysis of CT scans. For example, automated segmentation of CT scans can be

performed to identify 3D boundaries of specific organs (e.g., a prostate, lymph nodes, a lung or lungs), sub-organs, organ regions, as well as other regions of imaged tissue, such as particular bones and an overall skeletal region of the patient.

Ex1008, [0137]. Additionally, Baker discloses that “[a]utomated segmentation of CT scans can be accomplished via a variety of approaches, include [sic] machine learning techniques ... including, e.g., convolutional neural networks” Ex1008, [0137].

Baker further teaches that the patient’s 3D anatomical and functional images can be overlaid to form a composite image by establishing a mapping of coordinates and/or voxels of the two images that represent the same physical locations. *Id.* Thus, Baker states:

Once the 3D boundaries of various regions are identified within a CT scan of a composite image, by virtue of the mapping between the CT scan and PET scan of the composite image, the identified 3D boundaries can be transferred to the PET image. Accordingly, regions of the PET image falling within and/or outside of the identified 3D boundaries can be accurately identified.

Ex1008, [0138]. Consequently, “intensity values of the PET scan in relation to (e.g., within and/or outside of) the 3D boundaries of the identified regions can be used to determine levels of cancerous tissue within the identified regions, e.g., based on features of detected hotspots....” Ex1008, [0140].

4. The PROMISE Criteria (“Eiber”)

Eiber is a scientific journal article published in March 2018 in The Journal of Nuclear Medicine. Ex1009, p.469-470. An interested member of the public could have reasonably located this reference by searching jnm.snmjournals.org, the National Library of Medicine’s PubMed® database, or the article’s DOI reference. It is prior art under 35 U.S.C. §102(a)(1).

Eiber is directed to efforts to standardize reporting of prostate cancer nuclear medicine imaging results following the introduction of new prostate-cancer-specific radiotracers. Eiber explains: “Prostate-specific membrane antigen (PSMA)-ligand PET/CT or PET/MRI provides high sensitivity and specificity for prostate cancer staging. The accuracy of PSMA-ligand hybrid imaging is superior to that of conventional imaging and tracers.” Ex1009, p.469. Eiber also states: “We anticipate increased adoption of PSMA-ligand PET/CT fueled by upcoming evidence and inclusion into guidelines. Thus, reporting standards must be created now to aid reproducibility, enhance communication, and ultimately support acceptance of this technology.” *Id.* Accordingly, Eiber introduces the “Prostate Cancer Molecular Imaging Standardized Evaluation (PROMISE) criteria.” *Id.*

Eiber describes a standardized method of scoring individual lesions (i.e., hotspots) detected using PSMA PET by: (i) measuring the uptake (intensity) of a lesion; (ii) measuring the uptake in reference organs such as the liver; and (iii)

comparing the uptake in the lesion to the uptake in the reference organs to place the lesion on a scale relative to the reference organs, e.g., more or less uptake than the liver. For example, with reference to Table 1, which is reproduced below, Eiber states:

We propose a miPSMA score that enables standardized reporting of PSMA expression as detected with PSMA-ligand PET. Expression categories are defined in relation to mean uptake in the blood pool, liver, and parotid gland (Table 1; Fig. 1). Results are reported as 0, 1, 2, or 3 for no, low, intermediate, or high PSMA expression, respectively.

Ex1009, p.471.

TABLE 1
miPSMA Expression Score

Score	Reported PSMA expression	Uptake
0	No	Below blood pool
1	Low	Equal to or above blood pool and lower than liver*
2	Intermediate	Equal to or above liver* and lower than parotid gland
3	High	Equal to or above parotid gland

*For PSMA ligands with liver-dominant excretion (e.g., ¹⁸F-PSMA1007) spleen is recommended as reference organ instead of liver.

5. US2011/0007954 (“Suehling”)

Suehling is a United States patent application that published on January 13, 2011. Ex1006. It is prior art under 35 U.S.C. §102(a)(1) and (a)(2).

Suehling discloses a system for automatically detecting lesions in 3D medical images such as CT images or hybrid PET/CT images. Ex1006, Abstract, Fig. 1, [0006], [0025]. With reference to Figs. 1 and 2 below, Suehling receives a 3D medical image and automatically segments the image into lesion search regions corresponding to particular organs and bones, as well as search regions outside the organs and bones. Ex1006, [0007], [0026]-[0031].

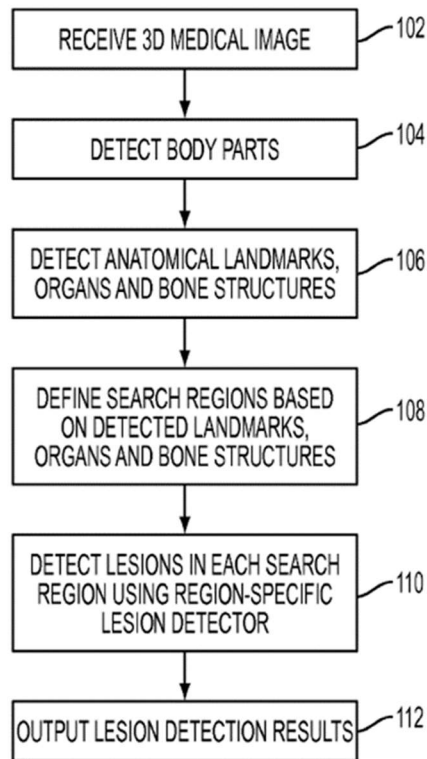


FIG. 1

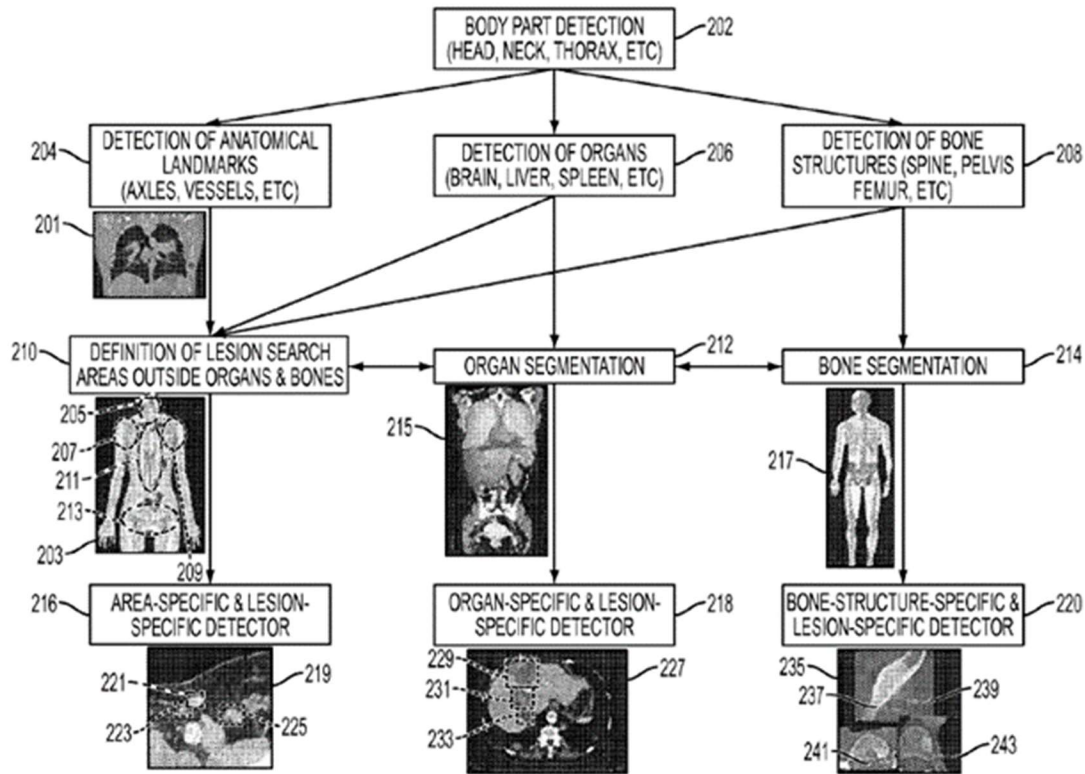


FIG. 2

Suehling teaches that “[a] general lesion detection algorithm for the whole body is ... unlikely to yield reliable results.” Ex1006, [0024]. Accordingly, Suehling detects lesions in each of the search regions, separately, using respective region-specific lesion detectors. Ex1006, [0032]-[0033].

B. Grounds A and B: Anticipation by Renisch or Obviousness over Renisch in view of Zhao

1. Claim 1: Method Claim

Claim 1 is anticipated by Renisch or obvious over Renisch-Zhao. Ex1002,

¶¶145-184.

- a) [1(pre)]³: “A method for automatically processing 3D images to automatically identify cancerous lesions within a subject, the method comprising:”

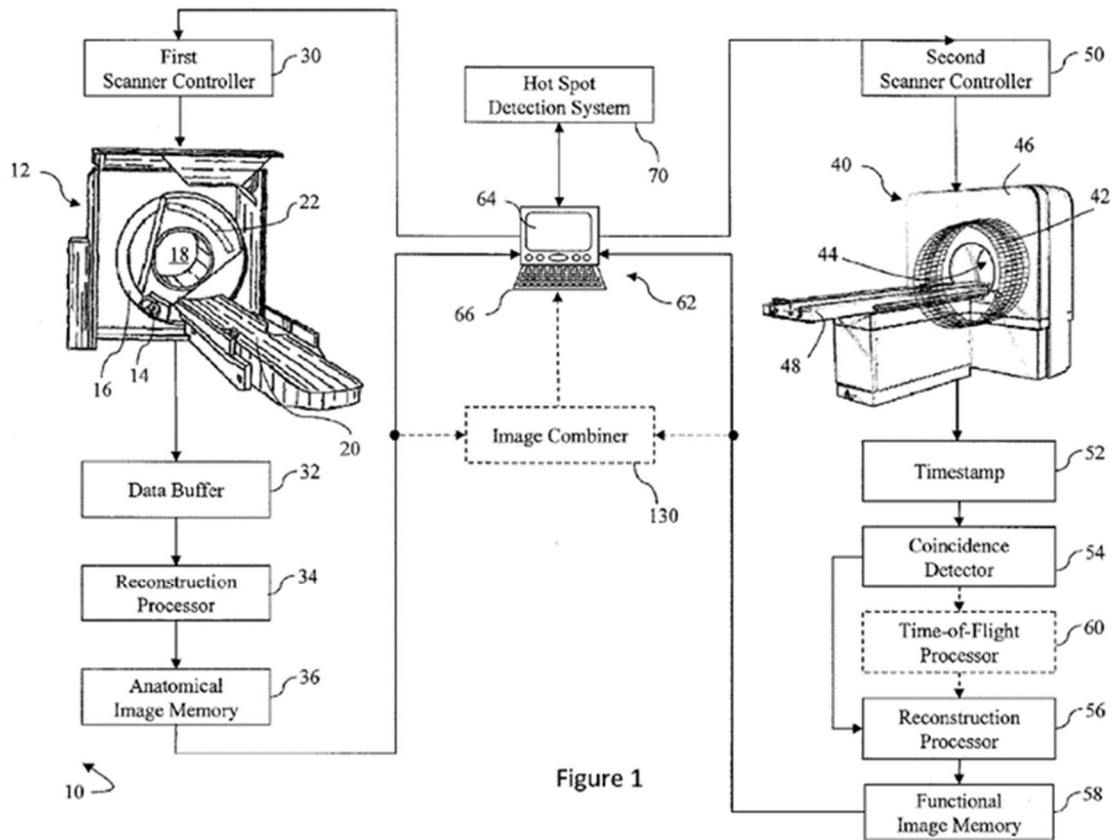
Renisch discloses the preamble if it is a limitation. Ex1005, Abstract, [0003], [0020]-[0023], [0029], [0032]; Ex1002, ¶¶145-150. Renisch teaches that regions of high radiotracer uptake, known as “hot spots,” may be cancerous lesions. Ex1005, [0003], [0029]. Renisch automatically analyzes 3D anatomical images (Ex1005, [0020]-[0021]) and 3D functional images (Ex1005, [0022]-[0023]) and discloses: “A hot spot detection system for automatically segmenting and quantifying hot spots in functional images” where “regions of high uptake are identified ... as one of potential lesions and non-potential lesions.” Ex1005, Abstract, [0032] (“perform various checks ... to determine if they are lesions”).

- b) [1(a)]: “receiving, by a processor of a computing device, a 3D anatomical image of a subject obtained using an anatomical imaging modality, wherein the 3D anatomical image comprises a graphical representation of tissue within the subject;”

Renisch discloses [1(a)]. Ex1005, Figs. 1-2, [0021], [0025]; Ex1002, ¶¶151-

³ The enclosed Claims Appendix includes the full claim language with bracketed reference characters identifying the respective limitations references in this Petition.

155. In Fig. 1 below, Renisch shows a diagnostic system 10 comprising an anatomical imaging scanner 12 (e.g., CT), a functional imaging scanner 40 (e.g., PET), a workstation/GUI 62, and an automatic hotspot detection system 70. *Id.* at [0020], [0022]. The anatomical imaging scanner 12 produces 3D anatomical images that provide a graphical representation of tissue within the patient/subject. Ex1005, [0020]-[0021].



Referring to Fig. 2 below, the hotspot detection system 70 comprises functional “units” that Renisch alternatively describes as “processors” or “algorithms” (i.e., stored instructions). *E.g.*, Ex1005, [0030] (“uptake unit,

processor, or algorithm 100”), [0031] (“classification unit, processor, or algorithm 101”).

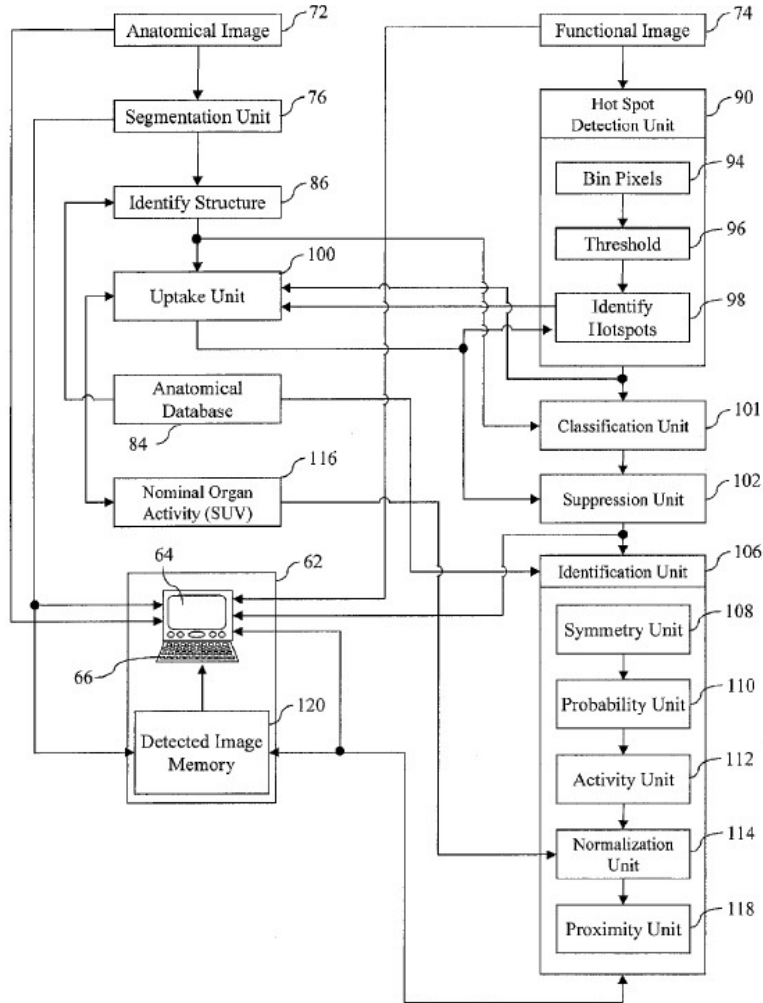


Figure 2

The hot spot detection system 70 performs “automatic detection of ... a lesion ... based on anatomical images 72 from the anatomical image memory 36 and functional images 74 from the functional image memory 58.” Ex1005, [0025]. As depicted in Fig. 2 above, the segmentation unit 76 (processor) receives the anatomical image 72, which is a reconstructed 3D image. Ex1005, [0021].

Accordingly, Renisch discloses [1(a)].

- c) **[1(b)]: “automatically identifying, by the processor, using one or more machine learning modules, for each of a plurality of target tissue regions, a corresponding target volume of interest (VOI) within the 3D anatomical image;”**

Renisch discloses [1(b)]. Ex1005, [0008] (“anatomical regions identified in the anatomical first image representation”), [0016] (“FIG. 3B illustrates anatomical structures segmented in an anatomical image representation”), [0025], [0027], [0038]; Ex1002, ¶¶156-158. Renisch states:

A segmentation unit 76 segments the anatomical first image representation 72 into regions which correspond to anatomical structures, particularly anatomical structures with high radiopharmaceutical tracer uptake which may obscure potential lesions of interest. In the case of FDG-PET, the brain 78, the heart 80, and the bladder 82 are organs of FIG. 3B which, when functioning normally, are examples of anatomical structures which often show high uptake unrelated to cancer. Other organs with high uptake include the kidneys and liver which are also contemplated for segmented anatomical structures.

Ex1005, [0025]. Thus, Renisch automatically segments, into volumes-of-interest, a plurality of predefined target tissue regions that correspond to organs that are expected to have high physiological uptake. Renisch further states:

The segmentation unit 76 is capable of employing different types of

segmentation methods. For example, the segmentation unit 76 can employ a model-based segmentation in which the central assumption is that the anatomical structures of interest have, to some extent, relatively consistent forms of geometry and position across patients. A library of three-dimensional anatomical structure models explaining the shape, geometrical location, size, and variations thereof are defined in an anatomical database 84 prior to the segmentation. During segmentation, the models act as templates to identify 86 and define the boundary of the structure of interest. It is to be appreciated, however, that other segmentation methods such as clustering, edge detection, region growing, principle components analysis, neural network, and the like are also contemplated.

Ex1005, [0027]. Both clustering and artificial neural networks are machine learning algorithms used for medical image segmentation tasks. Ex1002, ¶157 (citing Ex1016, pp.10-11). Thus, Rensich discloses [1(b)].

d) [1(c)]: “determining, by the processor, a 3D segmentation map representing a plurality of 3D segmentation masks, each 3D segmentation mask representing a particular identified target VOI;”

The Patent does not purport to have invented segmentation masks or the concept of a segmentation map. Limitation [1(c)] is merely an explicit statement of a routine implementation detail in digital image segmentation. Ex1002, ¶¶159-172.

(1) Anticipation by Renisch

Renisch discloses [1(c)] to a POSITA even though Renisch does not use the same terminology. Ex1005, [0025], [0027], [0030]-[0031], [0034], [0037], Figs. 3B and 3C; Ex1002, ¶¶163-167. Renisch segments a 3D anatomical image into multiple VOIs corresponding to different anatomical structures, such as the brain, heart, liver, and bladder. Ex1005, [0025], Fig. 3B. Each segmented VOI is represented by its own segmentation mask because, as explained below, each can be used *separately* to selectively suppress (or mask) uptake within corresponding volumes of a 3D functional image. Ex1005, [0030]-[0031].

After segmented organs are carried over from the anatomical image to the functional image, Renisch analyzes the uptake in each segmented organ to evaluate whether the organ is operating normally. Ex1005, [0030]. If an organ (e.g., the liver) is determined to be operating normally, the uptake in the organ is suppressed (i.e., filtered out) from the functional image and excluded from the search for potential lesions. Ex1005, [0031]. Thus, some segmented organs might be suppressed while others are kept for further analyses. Because Renisch discloses the functionality to separately suppress the uptake corresponding to each segmented organ, it is apparent that each segmented organ is represented by its own segmentation mask – even if not referred to as such. Ex1002, ¶165.

A “segmentation map,” as properly construed, is simply “a plurality of 3D

segmentation masks distinguishing a plurality of regions within a 3D image.” *See* Section VII.A. Therefore, the image segmentation results produced by Renisch are collectively a segmentation map representing a plurality of 3D segmentation masks, each mask representing a 3D segmented organ volume. Ex1002, ¶166. Accordingly, Renisch discloses [1(c)].

(2) Obviousness Over Renisch-Zhao

Additionally, or alternatively, Renisch-Zhao renders obvious this limitation because a POSITA would have been motivated to combine the references to arrive at the limitation. Ex1002, ¶¶168-172.

Zhao discloses [1(c)]: Zhao implements 3D medical image segmentation, like that discussed in Renisch, using segmentation masks. Ex1007, 5:11-6:11 (“segmentation may be implemented in medical image processing”) (“Such medical images may include ... CT.”) (“[A]n ROI may be an entire organ.”). Zhao states: “ROIs, once determined, may be represented by a digital mask containing a same number of pixels as the digital image” and “[a] digital mask may be alternatively referred [to] as a mask or a segmentation mask.” Ex1007, 5:25-29. Thus, Zhao discloses segmentation masks representing particular volumes-of-interest within 3D medical images, such as entire organs within CT images. Ex1002, ¶168.

Zhao also discloses the determination of a segmentation map representing a

plurality of segmentation masks. Ex1002, ¶169. Zhao states:

Each pixel of the mask may contain a value used to denote whether a particular corresponding pixel of the digital image is among any ROI, and if it is, which type of ROI among multiple types of ROIs does it fall. For example, if there is only a single type of ROI, a binary mask is sufficient to represent all ROIs. In particular, each pixel of the ROI mask may be either zero or one, representing whether the pixel is or is not among the ROIs. For a mask capable of representing multiple types of ROI, each pixel may be at one of a number of values each corresponding to one type of ROIs. A multi-value mask, however, may be decomposed into a combination [sic] the more fundamental binary masks each for one type of ROI.

Ex1007, 5:30-42 (emphasis added). The “multi-value mask” corresponds to a segmentation map, as claimed. Accordingly, Zhao discloses [1(c)].

Rationale to combine: Zhao is analogous art to Renisch. Both are directed to segmentation of 3D medical images, such as CT images, using neural networks. Ex1002, ¶170. *See, e.g.*, Ex1005, [0021], [0025], [0027]; Ex1007, 5:56-65, 6:4-11, 6:31-35.

A POSITA would have found it obvious, and been motivated, to implement the medical image segmentation described in Renisch using segmentation masks based on Zhao’s express teachings. Ex1002, ¶170. Renisch states generally that “[s]egmentation can ... be helpful for accurately determining a location of ... hot spots relative to the patient’s anatomy.” Ex1005, [0025]. Zhao expressly suggests

that ROI mask generation can be used in medical image processing for the same purpose. Ex1007, 5:56-6:11. Zhao states that medical image segmentation may produce “[o]ne or more ROI masks, alternatively referred to as segmentation masks” and that an “ROI mask may be used to mark the location of ... organ tissues and the regions outside of the ROI ... that are not part of the organ.” Ex1007, 6:1-7. Additionally, Zhao states that segmentation masks are particularly useful when processing digital images because “an ROI mask can be used as a filter to determine a subset of image data that ... need be further analyzed” while “[i]mage data outside these ... ROIs may be removed from further analysis.” Ex1007, 5:43-48. Accordingly, a POSITA would have been motivated to combine Renisch and Zhao based on Zhao’s express teaching and to better differentiate between regions located inside and outside of a segmented organ (e.g., by removing data outside the organ) to *better* determine the location of hotspots relative to a patient’s anatomy, as described in Renisch.

Alternatively, improving Renisch with the teachings of Zhao would merely have amounted to applying a known technique (segmentation masks) to a known device (Renisch) ready for improvement to yield predictable results. Renisch generally describes segmenting anatomical images into a plurality of anatomical regions and transferring those regions to functional images. If the Patent’s use of segmentation masks to perform this function is considered an improvement over

Renisch, then it would have been obvious to a POSITA to improve Renisch using Zhao. Zhao's technique for determining a 3D segmentation map representing a plurality of 3D segmentation masks is prior art to the Patent and is directly applicable to Renisch. Ex1002, ¶171. Zhao expressly states that its segmentation masks can be used to "mark the location of organ tissues," which is a critical task within Renisch. Ex1005, 6:1-7. Furthermore, Zhao explicitly states that "ROI masks are particularly useful for further processing" because "an ROI mask can be used as a filter." Ex1007, 5:43-45. Thus, a POSITA would have recognized that the result of applying Zhao to Renisch was predictable and would produce an improved system. Ex1002, 165.

Reasonable expectation of success: A POSITA would have had a reasonable expectation of success combining Renisch and Zhao in this manner since Zhao expressly applies to organ segmentation like that described in Renisch. Ex1002, ¶170.

- e) **[1(d)]: "receiving, by the processor, a 3D functional image of the subject obtained using a functional imaging modality;"**

Renisch discloses [1(d)]. Ex1005, Fig. 2 (functional image 74 being received by hotspot detection unit 90); Fig. 1 (functional image memory 58 connected to hot spot detection system 70 through workstation 62), [0022], [0025], [0029] ("a hot spot detection unit 90 detects from the functional second image

representation 74 regions of high intensity 92, depicted in FIG. 3A”); Ex1002, ¶¶173-175. Renisch includes a “functional imaging scanner 40” that produces “three-dimensional imaging data.” Ex1005, [0020]. Additionally, Renisch states that its automatic hotspot detection system, which includes a processor, detects lesions “based on anatomical images 72 from the anatomical image memory 36 and functional images 74 from the functional image memory 58.” Ex1005, [0025].

f) [1(e)]: “identifying, within the 3D functional image, one or more 3D volume(s), each corresponding to an identified target VOI, using the 3D segmentation map; and”

Renisch discloses [1(e)] or Renisch-Zhao renders obvious [1(e)] for the same reasons set forth in Section VIII.B.1.d) above. Ex1005, [0008], [0025], [0031], [0034], [0037], Figs. 3A-3C; Ex1002, ¶¶176-179.

For the reasons already explained in Section VIII.B.1.d), the plurality of segmented organs identified by Renisch from a 3D anatomical image constitute a segmentation map or, alternatively, Renisch-Zhao teaches a segmentation map. Renisch also discloses using those segmented organ volumes to identify corresponding volumes in a 3D functional nuclear medicine image (Ex1005, [0025], [0031]) stating that “anatomical regions identified in the anatomical first image representation could be carried over to the functional second image representation in order to delineate anatomical structures there.” Ex1005, [0008], [0034]. This description is essentially identical to the Patent, which states:

“Segmentation maps generated by automated AI-based analysis of anatomical images can be transferred to 3D functional images in order to identify, within the 3D functional image, 3D volumes corresponding to the target VOIs identified in the anatomical image.” Ex1001, 37:15-22. Thus, Renisch, or Renisch-Zhao, discloses [1(e)].

- g) [1(f): “automatically detecting, by the processor, within at least a portion of the one or more 3D volumes identified within the 3D functional image, one or more hotspots determined to represent lesions based on intensities of voxels within the 3D functional image.”**

Renisch discloses [1(f)]. Ex1005, [0025] (“automatic detection of a region of interest (ROI) pertaining to a lesion”), [0029]-[0032], Figs. 3A-3C (depicting highlight hotspots within segmented organ volumes); Ex1002, ¶¶180-183.

Renisch discloses a “hot spot detection unit 90” that automatically detects hotspots in 3D functional images based on the intensity values of voxels within the image. Ex1005, [0029]. The locations of the identified hotspots are compared with the locations of segmented organs to evaluate if the hotspots are lesions or just normal physiological uptake. Ex1005, [0030]-[0031]. Additionally, the uptake in the segmented organs is evaluated (e.g., for homogeneity) to determine if each organ is functioning normally. Ex1005, [0030]. “To improve detection of potential lesions, normally functioning anatomical structures are suppressed from the functional second image representation while unsuppressed regions ... of high

intensity are further analyzed to determine if they are plausible lesions. Ex1005, [0031]. Thus, a segmented organ that cannot be confirmed to be functioning normally, will be further examined to determine if the hotspots within the segmented organ are cancerous lesions. Ex1005, [0032]. Accordingly, Renisch discloses [1(f)].

Because Renisch discloses every limitation of claim 1, claim 1 is unpatentable as anticipated by Renisch. Alternatively, claim 1 is rendered obvious by Renisch-Zhao because it would be obvious to implement organ segmentation, as described in Renisch, using a plurality of segmentation masks as expressly taught by Zhao. Ex1002, ¶184.

2. Claim 2: “The method of claim 1, comprising using, by the processor, the one or more detected hotspots to determine a cancer status for the subject.”

Claim 2 depends from claim 1, which is anticipated by Renisch and/or rendered obvious by Renisch-Zhao. *See* Section VIII.B.1. Renisch also discloses the limitations of claim 2. Ex1005, [0032], [0034]; Ex1002, ¶¶185-187.

Renisch discloses an “identification unit, processor, or algorithm 106” that is “configured to calculate metrics corresponding to the unsuppressed regions [(i.e., hotspots)]” including “total tumor burden.” Ex1005, [0032]. Renisch also discloses a “probability unit, processor, or algorithm 112” that determines the likelihood that a lymph node is present in a high intensity region (i.e., hotspot),

which Renisch states “is a critical component in determining whether a tumor is likely to have metastasized, which dictates the therapeutic options for cancer patients.” Ex1005, [0034]. Thus, Renisch evaluates hotspots to: determine if they are cancer; determine if cancer has metastasized; and quantify total tumor burden.

Therefore, claim 2 is invalid as anticipated and/or obvious.

3. Claim 3

Claim 3 depends from claim 1, which is anticipated by Renisch and/or rendered obvious by Renisch-Zhao. *See* Section VIII.B.1. Renisch also discloses all the limitations of claim 3. Ex1002, ¶¶188-206.

- a) **[3(pre)]: “The method of claim 1, wherein the target tissue regions comprise one or more reference tissue regions and wherein the method comprises:”**

As already explained, Renisch automatically segments a plurality of predefined target tissue regions including the liver. Ex1005, [0025]. Renisch also states: “The metabolic activity of the liver can be used as a reference for comparison.” Ex1005, [0034].

- b) **[3(a)]: “using the 3D segmentation map to identify, by the processor, within the 3D functional image, one or more 3D reference volume(s), each corresponding to a particular reference tissue region;”**

As explained in Section VIII.B.1.d) above, Renisch discloses, or Renisch-Zhao teaches, a 3D segmentation map representing a plurality of segmented

organs. Renisch also discloses using the segmentation results to identify, within a 3D functional image, a 3D reference volume corresponding to the liver. Renisch states:

Since the liver is segmented and [identified] by the segmentation unit 76, an unsuppressed high intensity region can easily be compared to the uptake in the liver. Previously, a clinician had to manually delineate a region of the liver on a workstation which is time consuming and highly subjective. The anatomical regions identified in the anatomical first image representation 72 can be carried over to the functional second image representation 74 in order to delineate anatomical structures in the second image representation 74. The tracer uptake in these structures could be used as a reference for the quantification of the hot spots.

Ex1005, [0034].

Accordingly, Renisch discloses [3(a)]. Ex1002, ¶¶192-195.

- c) **[3(b)]: “determining, by the processor, one or more reference intensity values, each associated with a particular 3D reference volume of the one or more 3D reference volume(s) and corresponding to a measure of intensity within the particular 3D reference volume;”**

Renisch discloses [3(b)]. Ex1005, [0029], [0034]; Ex1002, ¶¶196-198.

Renisch identifies regions of high intensity in a 3D functional image by sorting the voxels of the image according to their grayscale values. Ex1005, [0029]. Renisch explains that these regions “can be caused by tumor growth” but “[t]hese regions

of high intensity also include normal functioning structures/organs such as the ... liver.” *Id.* Renisch states:

The metabolic activity of the liver can be used as a reference for comparison. Since the liver is segmented and [identified] by the segmentation unit 76, an unsuppressed high intensity region can easily be compared to the uptake in the liver.... The anatomical regions identified in the anatomical first image representation 72 can be carried over to the functional second image representation 74 in order to delineate anatomical structures in the second image representation 74. The tracer uptake in these structures could be used as a reference for the quantification of the hot spots, e.g. the relative activity of a hot spot compared with that of normal liver tissue could be computed.

Ex1005, [0034]. Thus, Renisch determines a reference intensity value based on the intensity within the identified liver volume.

- d) **[3(c)]: “determining, by the processor, one or more individual hotspot intensity values, each associated with a particular hotspot of at least a portion of the detected one or more hotspots and corresponding to a measure of intensity of the particular hotspot; and**

Renisch discloses [3(c)]. Ex1005, [0029], [0032], [0034]; Ex1002, ¶¶199-201. Renisch explains that regions of high intensity in functional images, generally referred to as “hot spots,” are identified by sorting the voxels of the image according to their grayscale values (i.e., intensity). Ex1005, [0029]. Renisch calculates metrics for identified hotspots including “SUV [standard uptake value],

average activity, maximum activity, minimum activity, homogeneity, and the like.” Ex1005, [0032]. Renisch also explains that individual hotspots can be quantified by comparison to normal organs, stating “the relative activity of a hot spot compared with that of normal liver tissue could be computed.” Ex1005, [0034].

- e) **[3(d)]: “determining, by the processor, one or more individual hotspot index values using the one or more individual hotspot intensity values and the one or more reference intensity values.”**

The Patent describes the determination of an individual hotspot index value as including the comparison of an individual hotspot intensity value to the intensity value of a reference region. Ex1001, 55:1-20.

Renisch discloses the same, stating:

A normalization unit, processor, or algorithm 114 compares the metabolic activity of an unsuppressed high intensity region with normally functioning structures, e.g. those identified by the uptake unit 100. For example, metabolic activity of a potential lesion is commonly compared to a standard uptake value determined by a nominal activity unit, processor, or algorithm 116.... The metabolic activity of the liver can be used as a reference for comparison. Since the liver is segmented and [identified] by the segmentation unit 76, an unsuppressed high intensity region can easily be compared to the uptake in the liver.... The anatomical regions identified in the anatomical first image representation 72 can be carried over to the functional second image representation 74 in order to delineate

anatomical structures in the second image representation 74. The tracer uptake in these structures could be used as a reference for the quantification of the hot spots, e.g. the relative activity of a hot spot compared with that of normal liver tissue could be computed.

Ex1005, [0034].

Accordingly, Renisch discloses [3(d)]. Ex1002, ¶¶202-206.

4. **Claim 4: “The method of claim 3, wherein the reference tissue regions comprise one or more members selected from the group consisting of: a liver, an aorta, and a parotid gland.”**

Claim 4 is anticipated by Renisch and/or rendered obvious by Renisch-Zhao for the same reasons provided in Section VIII.B.3 above. *See, e.g.*, Ex1005, [0034] (“The metabolic activity of the liver can be used as a reference for comparison.”); Ex1002, ¶¶207-208.

5. **Claim 5: “The method of claim 2, comprising, determining, by the processor, an overall index value indicative of a cancer status of the subject using at least a portion of the one or more hotspot index values.”⁴**

⁴ Claim 5 is invalid for anticipation or obviousness as written. However, Petitioner further submits that claim 5 contains a typographical error and actually depends from claim 3, not claim 2. The “hotspot index values” recited in claim 5 are introduced in claim 3, not claim 2. Thus, claim 5 should correctly read: “The method of claim 3,”

Claim 5 depends from claim 2, which is anticipated by Renisch and/or rendered obvious by Renisch-Zhao. *See* Section VIII.B.2. Renisch also discloses the additional limitations of claim 5. Ex1002, ¶¶209, 211.

As defined within the claim, the recited “overall index value indicative of a cancer status” can be determined using a single hotspot index value (i.e., a portion of “one or more”). *See also*, Ex1001, 38:1-9. As explained in Section VIII.B.3.e), Renisch determines individual hotspot index values by comparing their respective intensities to the intensity of a reference such as the liver. Accordingly, in the embodiment in which an overall index value is determined using a single hotspot index value, Renisch discloses claim 5. Thus, Renisch anticipates or Renisch-Zhao renders obvious claim 5. Ex1002, ¶211.

6. Claim 7: “The method of claim 1, wherein: the 3D anatomical image is an x-ray computed tomography (CT) image, and the 3D functional image is a 3D positron emission tomography (PET) image.”

Claim 7 depends from claim 1, which is anticipated by Renisch and/or rendered obvious by Renisch-Zhao. *See* Section VIII.B.1. Renisch also discloses the additional limitations of claim 7. Ex1002, ¶¶212-214.

Renisch discloses a diagnostic system 10 that includes a first imaging scanner 12 and a second imaging scanner 40. Ex1005, Fig. 1, [0020]-[0022]. The first imaging scanner may be “a computed tomography (CT) imaging scanner ...

for obtaining anatomical diagnostic images” using “an x-ray source.” Ex1005, [0020]. Renisch also explains that the CT scanner includes a processor that “reconstructs 3D image representations from the acquired imaging data.” Ex1005, [0021]. The second imaging system 40 may be a “PET scanner ... for obtaining functional images” and likewise acquires “three-dimensional imaging data” Ex1005, [0022].

7. Claim 19

Claim 19 depends from claim 1, which is anticipated by Renisch and/or rendered obvious by Renisch-Zhao. *See* Section VIII.B.1. Renisch also discloses all the limitations of claim 19. Ex1002, ¶¶231-240.

- a) **[19(pre)]: “The method of claim 1, wherein the target tissue regions comprise one or more background tissue regions and wherein the method comprises:”**

The Patent describes the “background tissue regions” as being “e.g., a background tissue region in which significant radiopharmaceutical uptake occurs under normal circumstances and is not necessarily indicative of presence of cancerous lesions.” Ex1001, 8:57-65. Examples of background tissue regions, according to the Patent, include “a bladder (e.g., a urinary bladder), a kidney, a duodenum, a small intestine, a spleen, a liver, a pancreas, a stomach, an adrenal gland, a rectum, and testes.” Ex1001, 18:48-52.

Renisch discloses these same features, stating:

A segmentation unit 76 segments the anatomical first image representation 72 into regions which correspond to anatomical structures, particularly anatomical structures with high radiopharmaceutical tracer uptake which may obscure potential lesions of interest. In the case of FDG-PET, the brain 78, the heart 80, and the bladder 82 are organs of FIG. 3B which, when functioning normally, are examples of anatomical structures which often show high uptake unrelated to cancer. Other organs with high uptake include the kidneys and liver which are also contemplated for segmented anatomical structures.

Ex1005, [0025]. Accordingly, Renisch discloses [19(pre)]. Ex1002, ¶¶232-233.

- b) [19(a)]: “at step (e), using the 3D segmentation map to identify, within the 3D functional image, as at least a portion of the one or more 3D volumes, one or more 3D background tissue volume(s), each corresponding [sic] a particular background tissue region; and”**

Renisch discloses, or Renisch-Zhao teaches, step (e) of claim 1 ([1(e)]). *See* Section VIII.B.1.f). Renisch also discloses the additional limitations of [19(a)] for the same reasons stated in the preceding Section. Ex1002, ¶¶234-235.

Renisch describes segmenting anatomical images into regions that correspond to anatomical structures, including anatomical structures with high radiopharmaceutical tracer uptake that is likely unrelated to cancer (e.g., the bladder and liver). Ex1005, [0025]. Renisch further discloses that “[t]he anatomical regions identified in the anatomical first image representation 72 can be

carried over to the functional second image representation 74 in order to delineate anatomical structures in the second image representation 74.” Ex1005, [0034].

- c) **[19(b)]: “excluding voxels of the 3D [sic] within the 3D background tissue from the voxels used to automatically detect the one or more hotspots at step (f).”**

“[T]he one or more hotspots” in [19(b)] refers back, for antecedent basis, to the “one or more hotspots determined to represent lesions” recited in step (f) of claim 1 ([1(f)]). Renisch discloses [1(f)], *i.e.*, “automatically detecting ... hotspots determined to represent lesions.” *See* Section VIII.B.1.g). Renisch also discloses the additional limitations of [19(b)]. Ex1005, [0031]-[0032]; Ex1002, ¶¶236-240.

Renisch automatically detects hotspots determined to represent lesions based on intensities of voxels in the functional image after suppressing from the functional image regions of high intensity in normally functioning organs that are expected to have high physiological uptake unrelated to cancer. Ex1005, [0025], [0031]-[0032]. For example, Renisch states:

[R]egions of high intensity that correspond to normally functioning anatomical structures may obscure potentially hazardous lesions. To improve detection of potential lesions, normally functioning anatomical structures are suppressed from the functional second image representation while unsuppressed regions 104, shown in FIG. 3C, of high intensity are further analyzed to determine if they are plausible lesions.

Ex1005, [0031]. Renisch automatically “perform[s] various checks on the unsuppressed regions 104 to determine if they are lesions.” Ex1005, [0032]. For example, Renisch states:

[A] symmetry unit, processor, or algorithm 108 determines symmetric pairs of the high intensity regions of the second and/or first image representation that correspond to paired anatomical structures. For example, if a high intensity region is identified, by the identification unit 98, as a salivary gland, the symmetry unit searches for the corresponding salivary gland on the other side of the patient. Activity patterns between the symmetric pairs are determined by an activity unit, processor, or algorithm 110. If an asymmetry of metabolic activity exists between the symmetric pair, the unsuppressed high intensity region 104 is identified as a potential lesion.

Ex1005, [0032]. Thus, Renisch automatically detects hotspots determined to be lesions based on intensities of voxels within the 3D functional image ([1(f)]) after first excluding high intensity voxels from the functional image that correspond to normally functioning high uptake organs ([19(b)]). Ex1002, ¶238.

8. Claims 10-14, 16, and 26: System Claims

Claim 10 recites a “system for automatically processing 3D images” that is substantively identical to the “method for automatically processing 3D images” recited in claim 1, addressed above. Whereas claim 1 (the method claim) recites a series of steps, each performed “by a processor,” claim 10 (the system claim)

recites a “processor” with stored instructions that perform the same steps recited in claim 1. Similarly, dependent claims 11-14, 16, and 26 are substantively identical to dependent claims 2-5, 7, and 19 discussed above.⁵ For those reasons discussed above and the additional reasons in the table below, Renisch or Renisch-Zhao render system claims 10-14, 16, and 26 unpatentable. Ex1002, ¶¶215-230, 241.

Limitation	Reasoning {referenced limitation}
[10(pre)]	<i>See</i> Section VIII.B.1.a) {[1(pre)]}
[10(i)]	<i>See</i> Section VIII.B.1.b) {[1(a)]}
[10(ii)]	<i>See</i> Section VIII.B.1.b) {[1(a)]}
[10(iii)]	<i>See</i> Section VIII.B.1.c) {[1(b)]}
[10(iv)]	<i>See</i> Section VIII.B.1.d) {[1(c)]}
[10(v)]	<i>See</i> Section VIII.B.1.e) {[1(d)]}
[10(vi)]	<i>See</i> Section VIII.B.1.f) {[1(e)]}
[10(vii)]	<i>See</i> Section VIII.B.1.g) {[1(f)]}
[11]	<i>See</i> Section VIII.B.2 {[2]}
[12(pre)]	<i>See</i> Section VIII.B.3.a) {[3(pre)]}
[12(a)]	<i>See</i> Section VIII.B.3.b) {[3(a)]}
[12(b)]	<i>See</i> Section VIII.B.3.c) {[3(b)]}
[12(c)]	<i>See</i> Section VIII.B.3.d) {[3(c)]}
[12(d)]	<i>See</i> Section VIII.B.3.e) {[3(d)]}
[13]	<i>See</i> Section VIII.B.4 {[4]}
[14]	<i>See</i> Section VIII.B.5 {[5]}
[16]	<i>See</i> Section VIII.B.6 {[7]}
[26(pre)]	<i>See</i> Section VIII.B.7.a) {[19(pre)]}
[26(a)]	<i>See</i> Section VIII.B.7.b) {[19(a)]}
[26(b)]	<i>See</i> Section VIII.B.7.c) {[19(b)]}

⁵ Similar to claim 5, claim 14 contains a dependency error as written. Whereas claim 5 should depend from claim 3, Petitioner submits that claim 14 should depend from claim 12, not claim 11.

C. Ground C and D, Obviousness over Renisch, or Renisch-Zhao, each in view of Baker or Eiber

- 1. Claim 8/17: “The [method/system] of claim [7/16], wherein the 3D PET image of the subject is obtained following administration to the subject of a radiopharmaceutical comprising a prostate-specific membrane antigen (PSMA) binding agent.”**

Claims 8 and 17 are identical but depend from claims 7 (Section VIII.B.6) and 16 (Section VIII.B.8), respectively, both which are anticipated by Renisch or rendered obvious by Renisch-Zhao. Claims 8 and 17 are rendered obvious by Renisch or Renisch-Zhao, each in view of Baker or Eiber. Ex1002, ¶¶242-249, 251.

Baker and Eiber each disclose [8]/[17]: Whereas Renisch describes the detection of cancer generally, Baker discloses that “[t]here are also a number of radiopharmaceuticals available for imaging particular kinds of cancer” including PSMA for prostate cancer. Ex1008, [0004], [0019], [0090], [0092]. For example, Baker states:

[An] example radiopharmaceutical is PyLTM (also known as [¹⁸F]DCFPyL, and 18F-PyL), which is a clinical-stage, fluorinated PSMA-targeted PET imaging agent for prostate cancer. A proof-of-concept study published in the April 2015 issue of the Journal of Molecular Imaging and Biology demonstrated that PET imaging with PyLTM showed high levels of PyLTM uptake in sites of putative metastatic disease and primary tumors, suggesting the potential for high sensitivity and specificity in detecting prostate cancer.

Ex1008, [0005]; *see also* Ex1001, 2:1-10 (applicant admitted prior art). Similarly, Eiber discloses that “[p]rostate-specific membrane antigen (PSMA)-ligand PET/CT ... provides high sensitivity and specificity for prostate cancer staging” and “[t]he accuracy of PSMA-ligand hybrid imaging is superior to that of conventional imaging and tracers.” Ex1009, p.469. Accordingly, a POSITA would have known that radiopharmaceuticals having PSMA binding agents existed for PET imaging before the Patent. Ex1002, ¶245.

Rationale to combine: Renisch, Baker, and Eiber are analogous art. Ex1002, ¶¶243-248. All relate to PET imaging for cancer evaluation.

Renisch discloses a system for imaging and analyzing cancerous lesions throughout the body and is not limited to any particular type of cancer or radiopharmaceutical. Renisch explains: “Typically, an object or patient to be imaged is injected with one or more radiopharmaceutical or radioisotope tracers and placed in the examination region” of a PET scanner. Ex1005, [0023]. “Examples of such tracers are 18F FDG, C-11, Tc-99m, Ga67, and In-111.” *Id.* A POSITA would recognize that Renisch could be useful for evaluating prostate cancer because the 18F FDG tracer, which is identified in Renisch, could be used to image many types of cancer, including prostate cancer. Ex1010 (“Iagaru”), [0004] (“(¹⁸F-FDG) positron emission tomography and computed tomography (PET/CT) is established as a powerful imaging tool for cancer detection.”), [0006]-

[0008], [0024] (describing the results of imaging prostate cancer using ¹⁸F-FDG PET), [0056] (“¹⁸F-FDG PET has limited ability to detect osseous metastatic lesions, but can still be useful in the detection of metastatic nodal and soft tissue disease.”), Table 1; Ex1002, ¶¶243-244.

A POSITA would have been motivated to use a radiopharmaceutical with a PSMA binding agent to image prostate cancer with the PET imaging system disclosed in Renisch based on the express teachings in either Baker or Eiber. Ex1002, ¶¶246, 248. It is general knowledge that prostate cancer is one of the most common forms of cancer among men. Ex1020, p.211; Ex1002, ¶244. Eiber teaches that PSMA PET imaging “provides high sensitivity and specificity for prostate cancer imaging” and “is superior to that of conventional imaging and tracers.” Ex1009, p.469. Similarly, Baker explains that one “PSMA-targeted PET imaging agent for prostate cancer,” PyL™, “showed high levels of ... uptake in sites of putative metastatic disease and primary tumors, suggesting the potential for high sensitivity and specificity in detecting prostate cancer.” These statements alone provide the express teaching and suggestion to use a PSMA binding agent with a PET system like Renisch.

Reasonable expectation of success: A POSITA would have had a reasonable expectation of success combining Renisch (or Renisch-Zhao) with either Baker or Eiber since the combinations merely involve a straightforward

substitution of one radiopharmaceutical, ^{18}F FDG, with a PSMA-based radiopharmaceutical – and using it for its intended purpose. Ex1002, ¶¶245-248. Indeed, as already stated above, both Baker and Eiber expressly state that PSMA PET imaging has been demonstrated to be successful.

2. Claims 9/18: “The [method/system] of claim [8/17], wherein the radiopharmaceutical comprises ^{18}F DCFPyL.”

Claims 9 and 18 depend from claims 8 and 17 (Section VIII.C.1), respectively, and add “wherein the radiopharmaceutical comprises ^{18}F DCFPyL,” which is also disclosed by both Baker (Ex1008, [0005], [0017], [0036], [0045], [0095]-[0096]) and Eiber (Ex1009, p, 472 (Fig. 1)). Accordingly, claims 9 and 18 are rendered obvious by Renisch, or Renisch-Zhao, each in view of Baker or Eiber for the same reasons previously stated in Section VIII.C.1 above. Ex1002, ¶¶250, 252.

3. Claim 22/29: “The [method/system] of claim [8/17], wherein the radiopharmaceutical comprises ^{68}Ga -PSMA-11.”

Claims 22 and 29 depend from claims 8 and 17 (Section VIII.C.1), respectively, and add “wherein the radiopharmaceutical comprises ^{68}Ga -PSMA-11,” which is also disclosed by both Baker (Ex1008, [0099]-[0100]) and Eiber (Ex1009, p.472 (Fig. 1)). Accordingly, claims 22 and 29 are rendered obvious by Renisch, or Renisch-Zhao, each in view of Baker or Eiber for the same reasons previously stated in Section VIII.C.1 above. Ex1002, ¶¶253, 257.

4. Claims 23/30: “The method of claim [8/17], wherein the radiopharmaceutical comprises ^{68}Ga -PSMA-617.”

Claims 23 and 30 depend from claims 8 and 17 (Section VIII.C.1), respectively, and add “wherein the radiopharmaceutical comprises ^{68}Ga -PSMA-617,” which is also disclosed by Baker. Ex1008, [0101]-[0102]. Accordingly, claims 23 and 30 are obvious over Renisch, or Renisch-Zhao, each in view of Baker for the same reasons previously stated in Section VIII.C.1 above. Ex1002, ¶¶254, 258.

5. Claims 24/31: “The method of claim [8/17], wherein the radiopharmaceutical comprises ^{68}Ga -PSMA-I&T.”

Claims 24 and 31 depend from claims 8 and 17 (Section VIII.C.1), respectively, and add “wherein the radiopharmaceutical comprises ^{68}Ga -PSMA-I&T,” which is also disclosed by both Baker (Ex1008, [0103]-[0104]) and Eiber (Ex1009, p.472 (Fig. 1)). Accordingly, claims 24 and 31 are obvious over Renisch, or Renisch-Zhao, each in view of Baker or Eiber for the same reasons previously stated in Section VIII.C.1 above. Ex1002, ¶¶255, 259.

6. Claims 25/32: “The method of claim [8/17], wherein the radiopharmaceutical comprises ^{18}F -PSMA-1007.”

Claims 25 and 32 depend from claims 8 and 17 (Section VIII.C.1), respectively, and add “wherein the radiopharmaceutical comprises ^{18}F -PSMA-1007,” which is also disclosed by both Baker (Ex1008, [0105]-[0106]) and Eiber

(Ex1009, p.472 (Fig. 1)). Accordingly, claims 25 and 32 are obvious over Renisch, or Renisch-Zhao, each in view of Baker or Eiber for the same reasons previously stated in Section VIII.C.1 above. Ex1002, ¶¶256, 260.

D. Ground E, Obviousness Over Baker in view of Zhao

1. Claim 1

a) [1(pre)]: Automatically processing 3D images to automatically identify cancerous lesions

Baker discloses “automatically analyzing ... one or more ... medical images[,] e.g., ... computed tomography (CT) images, ... to generate a risk map ... marking regions of risk of current disease ..., e.g., cancer.” Ex1008, [0032]. The CT images are 3D medical images. Ex1008, [0137] (“CT scans provide accurate anatomical information in the form of detailed three-dimensional (3D) images.”). Baker also states that hotspots are “automatically identified” (Ex1008, [0152]) and “classified as corresponding to cancerous lesions (e.g., metastases) (Ex1008, [0131]). Accordingly, Baker discloses [1(pre)]. Ex1002, ¶¶261-263.

b) [1(a)]: Receiving a 3D anatomical image

Baker discloses these limitations. Ex1002, ¶¶264-267. Baker states: “[T]he invention is directed to a method comprising ... receiving and storing, by a processor of a server computing device ... medical images []e.g., comprising ... computed tomography (CT) images.” Ex1008, [0032], [0036] (“the medical

images comprise ... a CT scan of the ... patient”). “The processor [] can process instructions for execution ... including instructions stored in [] memory.” Ex1008, [0165]. Additionally, Baker explains: “CT scans provide accurate anatomical information in the form of detailed three-dimensional (3D) images of internal organs, bones, soft tissue, and blood vessels.” Ex1008, [0137].

c) [1(b)]: Automatically identifying a target volume of interest within the 3D anatomical image using machine learning

Baker discloses this limitation. Ex1002, ¶¶268-271. Baker states:

[A]utomated segmentation of CT scans can be performed to identify 3D boundaries of specific organs (e.g., a prostate, lymph nodes, a lung or lungs) ... as well as other regions of imaged tissue, such as particular bones and an overall skeletal region of the patient. Automated segmentation of CT scans can be accomplished via a variety of approaches, include [sic] machine learning techniques [e.g., ANN-based approaches (including, e.g., convolutional neural networks (CNNs))].

Ex1008, [0137]. Baker’s automatic analysis includes “geographically identifying one or more organs ... and/or other regions of the imaged tissue” (Ex1008, [0032]) and the “[p]roperties of the one or more regions, such as their area or volume may ... be used” (Ex1008, [0132]).

d) [1(c)]: Determine a 3D segmentation map representing a plurality of 3D segmentation masks

Baker-Zhao renders [1(c)] obvious because a POSITA would have been motivated to combine the references to arrive at the limitation. Ex1002, ¶¶272-278. As already explained, Baker automatically segments an anatomical CT image into specific organ volumes. The respective 3D volumes are then transferred to a PET image by virtue of “mapping between the CT scan and PET scan.” Ex1008, [0138]. Baker does not use the term “segmentation mask,” but Zhao teaches and suggests the use of segmentation masks to implement 3D medical image segmentation like that discussed in Baker. Ex1007, 5:11-6:51.

Zhao discloses [1(c)]: As already explained in Section VIII.B.1.d)(2) above, Zhao discloses a segmentation map representing a plurality of segmentation masks as recited in [1(c)]. Ex1007, 5:11-6:11; Ex1002, ¶¶274-275.

Rationale to combine: Zhao and Baker are in the same field. Both are directed to segmentation of 3D medical images, such as CT images, using neural networks. Ex1002, ¶276. *See, e.g.,* Ex1008, [0137]; Ex1007, 5:56-65, 6:4-11, 6:31-35.

A POSITA would have found it obvious, and been motivated, to implement the organ segmentation described in Baker using segmentation masks based on Zhao’s express teachings. Ex1002, ¶276. Zhao states that medical image segmentation may produce “[o]ne or more ROI masks, alternatively referred to as segmentation masks” and that an “ROI mask may be used to mark the location of

... organ tissues and the regions outside of the ROI ... that are not part of the organ.” Ex1007, 6:1-7. Additionally, Zhao states that segmentation masks are useful because “an ROI mask can be used as a filter to determine a subset of image data” while “[i]mage data outside these ... ROIs may be removed from further analysis.” Ex1007, 5:43-48. Accordingly, a POSITA would have been motivated to combine Baker and Zhao based on Zhao’s express teaching and to better differentiate between regions located inside and outside of a segmented organ, e.g., by removing data outside the organ.

Alternatively, combining Baker with Zhao would merely have amounted to combining prior art elements (i.e., segmenting 3D medical images and generating digital masks of segmented ROIs) according to known methods (described in Zhao) to yield predictable results. Ex1002, ¶277. Baker describes segmenting a CT image into 3D organ volumes. Ex1008, [0137]. Zhao likewise describes segmenting organs in a medical image (Ex1007, 5:60-6:4) and further describes using segmentation results to generate a map comprising a plurality of binary “segmentation masks.” (Ex1007, 5:25-42). Thus, a POSITA could have predictably combined Baker and Zhao using the segmentation mask generating techniques described in Zhao without otherwise altering the functionality of Baker or Zhao. Ex1002, ¶277.

Reasonable expectation of success: A POSITA would have had a

reasonable expectation of success combining Baker and Zhao since Zhao expressly applies to organ segmentation like that described in Baker. Ex1002, ¶278.

e) [1(d)]: Receiving a 3D functional image

Baker discloses [1(d)]. Ex1008, [0017], [0032], [0036], [0139]; Ex1002, ¶¶279-280. Baker states:

[T]he invention is directed to a method comprising ... receiving and storing, by a processor of a server computing device ... medical images ... comprising one or more of the following: ... targeted PET images [or] targeted SPECT images ..., each medical image associated with a particular patient.”

Ex1008, [0032]. PET and SPECT images are reconstructed 3D images obtained using a functional (nuclear medicine) imaging modality. Ex1008, [0038] (“nuclear medicine image (e.g., a SPECT scan; e.g., a PET scan)”) (“geographically identify a 3D boundary ... within the nuclear medicine image”). Accordingly, Baker discloses [1(d)].

f) [1(e)]: Identifying a 3D volume within the 3D functional image using the 3D segmentation map

As explained in Section VIII.D.1.d), Baker-Zhao teaches a segmentation map representing a plurality of segmentation masks as recited in [1(c)]. Additionally, Baker describes using segmentation results to identify, within a 3D functional image, one or more 3D volume(s), each corresponding to an identified

target VOI in the anatomical image, as recited in [1(e)]. For example, Baker states: “Once the 3D boundaries of various regions are identified within a CT scan of a composite image, by virtue of the mapping between the CT scan and PET scan of the composite image, the identified 3D boundaries can be transferred to the PET image. Accordingly, regions of the PET image falling within and/or outside of the identified 3D boundaries can be accurately identified.” Ex1008, [0138], [0038] (“geographically identify a 3D boundary for each of one or more regions of imaged tissue [e.g., organs...] within the nuclear medicine image (e.g., such that portions of the nuclear medicine image falling within and/or outside of the 3D boundaries can be differentiated from each other)”). Accordingly, Baker-Zhao discloses [1(e)]. Ex1002, ¶¶281-283.

g) [1(f): Automatically detecting hotspots determined to represent lesions within the 3D volume identified within the 3D functional image

Baker discloses [1(f)]. Ex1008, [0032], [0038], [0039], [0129]-[0132], [0138], [0140], [0152] (“the automatically identified hotspots may be adjusted by the radiologist”); Ex1002, ¶¶284-289. Hotspots are localized regions of high intensity within functional images. Ex1008, [0131]. Baker expressly states that hotspots are “automatically identified.” Ex1008, [0152]. Baker also states: “Hotspots may be detected and/or classified as corresponding to cancerous lesions (e.g., metastases) using a variety of approaches, including, as described in U.S. Pat.

No. 8,855,387,” which Baker incorporates by reference in its entirety. Ex1008, [0131], [0129] (“U.S. Pat. No. 8,855,387 ... is incorporated herein by reference in its entirety.”) U.S. Patent No. 8,855,387 (Ex1014) describes detection of hotspots by thresholding images to identify pixels/voxels above a certain threshold intensity. Ex1014, 5:27-38.

With respect to detecting hotspots determined to be lesions within one or more identified 3D volumes, Baker states:

[O]nce the 3D boundaries of the various regions are identified within the PET scan, one or more risk indices can be computed.... In particular, in certain embodiments, intensity values of the PET scan in relation to (e.g., within and/or outside of) the 3D boundaries of the identified regions can be used to determine levels of cancerous tissue within the identified regions, e.g., based on features of detected hotspots (e.g., detected hotspots corresponding to metastases).

Ex1008, [0140]. Accordingly, Baker automatically detects hotspots determined to represent cancerous lesions based on the intensities of voxels within a 3D functional image. Additionally, Baker discloses detecting these hotspots within 3D volumes identified within the 3D functional image (e.g., the skeleton).

2. Claim 2: Using hotspots to determine cancer status

Claim 2 depends from claim 1, which is obvious over Baker-Zhao. *See* Section VIII.D.1. Baker also discloses the limitations of claim 2. Ex1008, [0039],

[0053], [0131], [0152]; Ex1002, ¶¶291-293.

As already explained, Baker automatically detects hotspots and classifies them as cancerous lesions or not. Ex1008, [0152] (“automatically identified hotspots”), [0131] (“Hotspots may be ... classified as corresponding to cancerous lesions.”). Baker also automatically computes risk indices based on the number or volume of hotspots within one or more tissue regions (Ex1008, [0039]) and tracks cancer progression using the risk indices, where the values of the risk indices correspond to “numeric values identifying a particular cancer stage” (Ex1008, 0053).

Accordingly, Baker-Zhao renders claim 2 obvious under the same rationale expressed in Section VIII.D.1 above.

3. Claim 7: Computed tomography (CT) and positron emission tomography (PET) images

Claim 7 depends from claim 1, which is obvious over Baker-Zhao. Baker also discloses the additional limitations recited in claim 7. Ex1008, [0032], [0036], [0038], [0136]-[0140]; Ex1002, ¶¶294-295. Baker states:

In certain embodiments, the medical images comprises a positron emission tomography (PET) scan of a first patient obtained following administration to the first patient of an imaging agent comprising [18F]DCFPyL (DCFPyL labeled with ¹⁸F), and a CT scan of the first patient, wherein the method comprises overlaying the PET scan with the CT scan to create a composite image (PET-CT) of the first patient.

Ex1008, [0036]. Accordingly, Baker-Zhao renders claim 7 obvious under the same rationale expressed for claim 1.

4. Claim 8: PET image obtained following administration of PSMA

Claim 8 depends from claim 7, which is obvious over Baker-Zhao. *See* Section VIII.D.3. Baker also discloses all the limitations of claim 8. *See* Section VIII.C.1; Ex1008, [0036], Ex1002, ¶¶296-297.

5. Claims 9 and 22-25: Specific radiopharmaceuticals

Claims 9 and 22-25 depend from claim 8, which is obvious over Baker-Zhao. *See* Section VIII.D.4. Baker also discloses all the limitations of claim 9 (Section VIII.C.2), claim 22 (Section VIII.C.3), claim 23 (Section VIII.C.4), claim 24 (Section VIII.C.5), and claim 25 (Section VIII.C.6). Ex1002, ¶¶298, 314-317. Accordingly, Baker-Zhao also renders obvious claims 9 and 22-25.

6. Claims 10-11, 16-18, and 29-32

As already explained in Section VIII.B.8 above, system claim 10 is substantively identical to method claim 1, addressed above. Similarly, dependent claims 11, 16-18, and 29-32 are substantively identical to dependent claims 2, 7-9, and 22-25 discussed above. For those reasons discussed above and the additional reasons in the table below, Baker-Zhao renders system claims 10-11, 16-18, and 29-32 unpatentable. Ex1002, ¶¶299-313, 318-321.

Limitation	Reasoning {referenced limitation}
[10(pre)]	<i>See</i> Section VIII.D.1.a){[1(pre)]}
[10(i)]	<i>See</i> Section VIII.D.1.b){[1(a)]}
[10(ii)]	<i>See</i> Section VIII.D.1.b){[1(a)]}
[10(iii)]	<i>See</i> Section VIII.D.1.c){[1(b)]}
[10(iv)]	<i>See</i> Section VIII.D.1.d){[1(c)]}
[10(v)]	<i>See</i> Section VIII.D.1.e){[1(d)]}
[10(vi)]	<i>See</i> Section VIII.D.1.f){[1(e)]}
[10(vii)]	<i>See</i> Section VIII.D.1.g){[1(f)]}
[11]	<i>See</i> Section VIII.D.2){[2]}
[16]	<i>See</i> Section VIII.D.3){[7]}
[17]	<i>See</i> Section VIII.D.4){[8]}
[18]	<i>See</i> Section VIII.D.5){[9]}
[29]	<i>See</i> Section VIII.D.5){[22]}
[30]	<i>See</i> Section VIII.D.5){[23]}
[31]	<i>See</i> Section VIII.D.5){[24]}
[32]	<i>See</i> Section VIII.D.5){[25]}

E. Ground F, Obviousness over Baker-Zhao in view of Eiber

1. Claim 3/12

Claims 3 (method) and 12 (system) are substantively the same but depend from claims 1 and 10, respectively. Whereas claim 3 recites a series of steps performed “by the processor,” claim 12 refers to instructions that “cause the processor to” perform the same steps recited in claim 3.

Claims 1 (method) and 10 (system) are both obvious over Baker-Zhao. *See* Sections VIII.D.1 and VIII.D.6. Whereas these claims are directed to detecting hotspots determined to represent lesions based on their intensities, claims 3 and 12 add the concept of determining hotspot index values based on a detected hotspot’s

intensity and the intensity of a reference volume. This additional feature is explicitly recommended by Eiber (Ex1009) for prostate cancer evaluation like that described in Baker. Accordingly, claims 3 and 12 are rendered obvious by Baker-Zhao in further view of Eiber. Ex1002, ¶¶322-340, 342.

Rationale to combine: As explained in Section VIII.A.4 above, Eiber introduced the PROMISE criteria in 2018 to standardize the reporting of prostate cancer evaluations. The Patent essentially restates the PROMISE criteria without attributing it to Eiber. Ex1001, 4:4-40, 58:31-59.

It would have been obvious to a POSITA to practice the PROMISE method using the system and method disclosed by Baker-Zhao based on the express motivation, teaching, and suggestion provided in Eiber. Ex1002, ¶326. Baker discloses a system for automatically identifying cancerous lesions in a subject, including lesions representing prostate cancer detected using PSMA-ligand PET. Ex1008, [0092], [0136]-[0140]. Eiber provides the express teaching to report lesions detected with PSMA PET in a standardized manner to “aid reproducibility” and “enhance communication” because “[p]recise description and organized classification of PSMA-ligand PET/CT findings are needed.” Ex1009, p.469. Accordingly, it would have been obvious combine Baker-Zhao with Eiber and to characterize detected lesions by comparing them to uptake in a reference organ, as proposed by Eiber.

Reasonable expectation of success: Baker teaches automatic segmentation of anatomical regions, including the liver and lymph nodes, which are transferred to a functional image so that the uptake within the 3D boundaries of the segmented regions can be evaluated. Ex1008, [0137]-[0140]. It would have been straightforward for a POSITA to use the *already measured* uptake in the liver as a reference value for comparison detected hotspots, as taught by Eiber. Ex1002, ¶327.

All elements disclosed: As detailed below, the combination of Baker-Zhao with Eiber teaches all limitations of claim 3.

a) [3(pre)]/[12(pre)]: Reference tissue regions

As already explained in Section VIII.D.1.c), Baker automatically segments anatomical images to identify 3D boundaries for target tissue regions, including the liver. Ex1008, [0038]. Eiber uses measured uptake in the liver as a reference. Ex1009, p.471. Thus, Baker-Zhao with Eiber discloses [3(pre)]/[12(pre)] based on the explicit teachings in Eiber. Ex1002, ¶¶329-331.

b) [3(a)]/[12(a)]: Use segmentation map to identify a 3D reference volume within the 3D functional image

As explained in Section VIII.D.1.d) above, Baker-Zhao teaches a 3D segmentation map. Additionally, Baker identifies one or more tissue regions in a 3D functional image using its segmentation results. Ex1008, [0138]. Thus, Baker-Zhao renders obvious: “using the 3D segmentation map to identify, by the

processor, within the 3D functional image, one or more 3D ... volume(s).”
Ex1002, ¶332.

As explained in the preceding Section, it would be obvious to use one or more of the segmented tissue regions identified by Baker (e.g. liver and lymph nodes) as a reference tissue region, as expressly taught by Eiber. Accordingly, Baker-Zhao with Eiber teaches [3(a)]/[12(a)]. Ex1002, ¶333.

c) [3(b)]/[12(b)]: Determine a reference intensity value associated with the 3D reference volume

Baker automatically computes one or more risk indices based on the intensity values of a 3D functional image within one or more identified 3D boundaries. Ex1008, [0140]. Thus, Baker already measures intensity within 3D segmented volumes. Eiber teaches determining reference intensity values corresponding to the measured intensity within particular reference volumes of a functional image, including the heart, liver, and parotid gland. Ex1009, p.471. Thus, Baker-Zhao with Eiber – by using one of Baker’s segmented 3D volumes as a “3D reference volume” – teaches [3(b)]/[12(b)]. Ex1002, ¶334.

d) [3(c)]/[12(c)]: Determine individual hotspot intensity values

The Patent uses “intensity” and “SUV” interchangeably. *See, e.g.*, Ex1001, 58:31-59 (“intensity (SUV)”) (“blood and liver reference intensities (SUVs)”). Baker and Eiber both disclose [3(c)]/[12(c)]. Baker determines “an average

intensity of detected hotspots, a maximal intensity of detected hotspots, and the like.” Ex1008, [0132]. Eiber states: “[W]e advise comparison of the mean SUVs of the respective lesions and the reference organ.” Thus, both Baker and Eiber disclose [3(c)]/[12(c)]. Ex1002, ¶¶335-336.

e) **[3(d)]/(12(d)): Determine individual hotspot index values using the hotspot intensity values and the reference intensity value**

Baker-Zhao in combination with Eiber teaches [3(d)]/[12(d)]. Ex1002, ¶¶337-339, 344. Baker automatically calculates risk index values using a processor. Ex1008, [0038] (automatically analyzing an image by computing risk indices), [0132], [0140], [0164] (“computing device 800 ... can be used in the methods and systems described in this disclosure”), [0165] (“computing device 800 includes a processor 802”). Baker does not, however, calculate individual hotspot index values using individual hotspot intensity values and reference intensity values. Eiber teaches these limitations.

Eiber teaches PSMA “expression categories” (“PSMA score”) for individual lesions that are defined in relation to the measured uptake in the blood pool, liver, and parotid gland. Ex1009, p.471. Through “comparison of the mean SUVs of the respective lesions and the reference organ” Eiber determines individual hotspot index values, e.g., “0, 1, 2, or 3 for no, low, intermediate, or high PSMA expression.” Ex1009, p. 471, Table 1.

For reasons already stated above, it would have been obvious to a POSITA to determine individual hotspot index values, as claimed, using Baker's processor, based on the express motivation, teaching, and suggestion in Eiber. Ex1002, ¶339. Moreover, the additional task of calculating individual hotspot index values with Baker's processor would be straightforward using hotspot intensities and the intensity within the segmented liver, which are already determined by Baker.

2. Claims 4/13: Reference tissue regions selected from liver, aorta, and parotid gland

Claims 4 and 13 depend from claims 3 and 12, respectively, which are both rendered obvious by Baker-Zhao in further view of Eiber. *See* Section VIII.E.1. Eiber also discloses every element of claims 4 and 13 because, as already explained, Eiber uses the liver, a blood pool located in the aorta, and the parotid gland as reference tissue regions. Ex1009, p.471. Accordingly, Baker-Zhao in further view of Eiber renders obvious claims 4 and 13 for the same reason stated in Section VIII.E.1 above. Ex1002, ¶¶ 341, 345.

3. Claims 5/14: Overall index value indicative of cancer status

Claims 5 and 14, as drafted, depend from claims 2 and 11, respectively, which are both rendered obvious by Baker-Zhao. Eiber discloses the additional limitations of [5]/[14] and would be obvious to combine with Baker as explained in Section VIII.E.1.

As explained in Section VIII.E.1.e), Eiber determines individual hotspot

index values referred to as “PSMA scores.” Ex1009, pp.470-471. Eiber also uses one or more of the PSMA scores to determine cancer status (positive/negative). Ex1009, p.472-473 (Fig. 2). Thus, Eiber discloses [5]/[14]. Ex1002, ¶342. Alternatively, it would be obvious to a POSITA to represent cancer status (positive/negative) using index values (e.g., 1/0, respectively). Ex1002, ¶343. Accordingly, Baker-Zhao in further view of Eiber renders obvious claims 5 and 14. Ex1002, ¶¶342-343, 346.

F. Ground G, Obviousness over Baker-Zhao in view of Suehling

1. Claims 19/26

Claims 19 (method) and 26 (system) are substantively the same except that they depend from claims 1 and 10, respectively. Even a typographical error in claim 19 has been carried over to claim 26. Whereas claim 19 recites a series of method steps, claim 26 refers to instructions that “cause the processor to” perform the same steps recited in claim 19.

Independent claims 1 (method) and 10 (system) are both obvious over Baker-Zhao. *See* Sections VIII.D.1 and VIII.D.6. Claims 19 and 26 are rendered obvious by Baker-Zhao in further view of Suehling. Ex1002, ¶¶347-366. As detailed below, the combination of Baker-Zhao and Suehling teach every claim limitation.

a) [19(pre)]/[26(pre)]: Background tissue regions

The Patent describes “background tissue regions” as being “e.g., a background tissue region in which significant radiopharmaceutical uptake occurs under normal circumstances and is not necessarily indicative of presence of cancerous lesions.” Ex1001, 8:57-65. Examples of background tissue regions, include “a bladder (e.g., a urinary bladder), a kidney, a duodenum, a small intestine, a spleen, a liver, a pancreas, a stomach, an adrenal gland, a rectum, and testes.” Ex1001, 18:48-52.

Baker states: “[A]utomated segmentation of CT scans can be performed to identify 3D boundaries of specific organs (e.g., a prostate, lymph nodes, a lung or lungs) ... as well as other regions of imaged tissue, such as particular bones and an overall skeletal region of the patient.” Ex1008, [0137]. Additionally, Baker describes segmenting the liver (Ex1008, [0038]), which the Patent lists among the examples of background tissue regions (Ex1001, 7:65-8:2). Thus, Baker discloses [19(pre)]/[26(pre)]. Ex1002, ¶¶348-353.

b) [19(a)]/[26(a)]: Use the segmentation map to identify a 3D background tissue volume within the 3D functional image

As just explained, Baker segments target tissue regions in 3D anatomical images into organ volumes, including the liver, which the Patent lists as an example of a background tissue region. As explained in Sections VIII.D.1.d) and

VIII.D.1.f) above, Baker-Zhao also teaches transferring the segmented organ volumes from the anatomical image to a 3D functional image using a segmentation map. Accordingly, Baker-Zhao discloses [19(a)]/[26(a)]. Ex1002, ¶¶354-355.

c) [19(b)]/[26(b)]: Exclude voxels within the 3D background tissue from voxels used to automatically detect hotspots

Although Baker automatically identifies background tissue volumes (e.g., the liver) in the 3D functional image, Baker does not describe excluding voxels within these regions from the voxels used to automatically detect hotspots. Suehling discloses this limitation.

As described in Section VIII.A.5 above, Suehling receives one or more 3D medical images (Ex1006, [0025], Fig. 1 (102)) and automatically segments them into lesion search regions (Ex1006, [0026]-[0028]) correspond to particular organs and bones such as the brain, liver, spleen, kidneys, and spine (Ex1006, [0007], [0027]). The one or more images can be an anatomical CT image or a composite PET/CT image, for example. Ex1006, [0025], [0036].

Each distinct search region defined by Suehling is searched *separately* using “a separate region-specific detector ... trained based on annotated training data for each region.” Ex1006, [0033]. Thus, for each region (e.g., organ), the voxels of the image outside the region (i.e., the background) are exclude from the search. For example, when defining the “specific search areas for lymph nodes,” Suehling

states that the segmented organs and bones are used “to exclude the detected organs and bones from these search regions.” Ex1006, [0029]. Likewise, Suehling describes using a “trained region-specific detector” based on “marginal space leaning (MSL)” to search for lesions in each respective search region, and expressly states “MSL is applied to the restricted search space.” Ex1006, [0032]. Accordingly, Suehling teaches excluding voxels (e.g., outside the search region) from the voxels used to automatically detect lesions (e.g., within the search region) as claimed. Ex1002, ¶¶357-360.

Additionally, as mentioned above, Suehling discloses embodiments in which composite images, such as PET/CT images, are searched for lesions. Ex1006, [0025], [0036]. In fact, Suehling teaches that “[t]he information of two imaging modalities may further improve the accuracy and robustness of the detection.” Ex1006, [0036]. Thus, for embodiments in which Suehling uses region-specific detectors to search for lesions in composite images, Suehling also excludes voxels of a 3D functional image (e.g., PET) from the voxels used to automatically detect lesions, as claimed.

Accordingly, Suehling discloses [19(b)]/[26(b)]. Ex1002, ¶¶358-360. Alternatively, Baker in view of Suehling teaches [19(b)]/[26(b)] since Baker searches 3D volumes in functional images for lesions and Suehling teaches to search each region separately using region-specific detectors. Ex1002, ¶¶361-364.

Rationale to combine: Although Baker describes segmenting one or more specific tissue regions and “determine[ing] levels of cancerous tissue within the identified regions,” (Ex1008, [0140]), Baker does not describe using different search criteria to identify lesions within respective regions. Nor, therefore, does Baker describe restricting its lesion search to particular regions or excluding certain voxels from the voxels used to automatically search for lesions.

Suehling teaches the advantage of region-specific detectors and, therefore, restricted search areas. Suehling states that “[a] general lesion detection algorithm for the whole body is ... unlikely to yield reliable results” because “the appearance of the same lesion entity may differ between different body regions.” Ex1006, [0024]. Accordingly, Suehling suggests “us[ing] body-region-specific detectors that exploit the typical context of a given region to detect lesions.” *Id.*

Accordingly, Suehling supplies the teaching, suggestion, or motivation that would have led a POSITA to combine Baker-Zhao with Suehling to arrive at the claimed invention. Whereas Baker is already concerned with determining cancerous tissue levels within particular tissue regions (e.g., the skeleton or prostate) for the purpose of computing risk indices, Suehling discloses a technique for improved lesion detection within such tissue regions using trained region-specific detectors. Accordingly, a POSITA would have been motivated to improve Baker based on the teachings in Suehling. Ex1002, ¶363.

Reasonable expectation of success: Additionally, a POSITA would have had a reasonable expectation of success combining Baker-Zhao with Suehling as proposed. Each of Baker, Zhao, and Suehling are in the same field of 3D medical image analysis using machine learning to segment specific tissue regions. Baker already uses the segmented tissue regions to identify and quantify lesions within respective regions of a functional image. Under the proposed combination Baker would also use different region-specific lesion search criteria in each region, as taught by Suehling. This could easily be accomplished based on the teachings of Zhao, which describes the use of segmentation masks produced from image segmentation like Baker and Suehling. Zhao states, for example, “an ROI mask can be used as a filter to determine a subset of image data ... that need be further analyzed and processed.” Using the teachings of Zhao and Suehling, a POSITA could have easily used a segmentation mask to exclude voxels outside of a specific tissue region (e.g., skeleton) so as to apply a region-specific detector to voxel within the regions, as taught by Suehling. Ex1002, ¶364.

Accordingly, Baker-Zhao in view of Suehling renders obvious claims 19 and 26.

2. Claim 28: “The system of claim 26, wherein the particular target tissue region is selected from the group consisting of: a skeletal region comprising one or more bones of the subject, a lymph region, and a prostate region.”⁶

Claim 28 depends from claim 26, which is obvious over Baker-Zhao in view of Suehling. *See* Section VIII.F.1. Baker and Suehling each disclose the additional limitation of claim 28. Ex1002, ¶¶367-370. As discussed *supra* Section VIII.F.1.a), Baker states that “automated segmentation of CT scans can be performed to identify 3D boundaries of specific organs” including “a prostate” and “lymph nodes,” “as well as other regions of imaged tissue, such as particular bones and an overall skeletal region of the patient.” Ex1008, ¶ [0137]. Likewise, Suehling states that its “automatic lesion detection method ... can be used to detect lesions in various parts of the body including ... lymph nodes ... and bone structures.” Ex1006, [0021]. As discussed in Section VIII.F.1.c), each distinct search region defined by Suehling is searched *separately* using “a separate region-specific detector ... trained based on annotated training data for each region.” Ex1006,

⁶ Claim 28 is invalid for obviousness as written. However, Petitioner further submits that claim 28 contains a typographical error and actually depends from claim 27, not claim 26. First, “the particular target tissue region” recited in claim 28 lacks antecedent basis in claim 26, but “a particular target tissue region” is introduced in claim 27. Furthermore, claims 27 and 28 add substantially the same limitations as claims 20 and 21, respectively, where claim 21 depends from claim 20. Thus, claim 28 should correctly read as “The system of claim 27, wherein”

[0033]. Thus, for each region (e.g., organ), the voxels of the image outside the region (i.e., the background) are excluded from the search. For example, when defining the “specific search areas for lymph nodes,” Suehling states that the segmented organs and bones are used “to exclude the detected organs and bones from these search regions.” Ex1006, [0029]. Thus, Baker-Zhao in view of Suehling renders obvious this claim.

IX. INSTITUTION IS APPROPRIATE

As explained in Section 0, Petitioner presents substantially different prior art combinations and arguments than those previously considered by the Office. 35 U.S.C. §325(d); *Advanced Bionics, LLC v. MED-EL Elektromedizinische Gerate GmbH*, IPR2019-01469, Paper 6 at 7-10 (PTAB Feb. 13, 2020) (precedential). Although some of Petitioner’s principal prior art was disclosed to the Office, it appears to have not been properly considered as evidenced by the Examiner stating that Hamadeh was the closest prior art. Other principle prior art—Zhao (Ex1007)—was not considered and speaks directly to “segmentation masks” as found in each independent claim of the Patent. Thus, even if Petitioner’s primary references had been properly considered—which they were not—the Petition sets forth new combinations that were not previously presented or cumulative. *See, e.g., Verizon Connect Inc. v. Omega Patents, LLC*, IPR2023-01163, Paper 12, p.14 (Feb. 21, 2024) (“[A]lthough we agree that Flick ’885 was previously presented to

the Office, we determine that the combination of Flick '885 and Flick '561 was not previously presented. Consequently, we determine that the same or substantially the same prior art or arguments were not previously presented to the Office, and we decline to exercise our discretion under §325(d) to deny institution of trial.”)

In accordance with the Interim Processes for PTAB Workload Management announced by USPTO Acting Director Stewart on March 26, 2025, if Patent Owner files a supplemental brief urging discretionary denial on any basis, Petitioner intends to file an opposition brief with additional analysis supporting its positions.

X. CONCLUSION

In light of the strength of the identified grounds, the Board should institute review of the challenged claims.

* * *

Date: April 4, 2025

By: / Jeffrey C. Metzcar /
Jeffrey C. Metzcar
Registration No. 52,027
THOMPSON HINE LLP
10050 Innovation Drive, Suite 400
Dayton, OH 45342

David R. Jaglowski
Registration No. 58,514
THOMPSON HINE LLP
41 South High Street, Suite 1700
Columbus, Ohio 43215

Marla R. Butler
THOMPSON HINE LLP
Two Alliance Center
3560 Lenox Road, NE., Suite 1600
Atlanta, GA 30326-4266

Jesse Jenike-Godshalk
THOMPSON HINE LLP
312 Walnut Street, Suite 2000
Cincinnati, OH 45202

James A. Rollins
Registration No. 82,811
THOMPSON HINE LLP
Two Alliance Center
3560 Lenox Road, NE., Suite 1600
Atlanta, GA 30326-4266

CERTIFICATION UNDER 37 C.F.R. § 42.24(D)

Pursuant to 37 C.F.R. §42.24(a)(1)(i), I certify that this paper includes 13,608 words. In accordance with 37 C.F.R. §42.24(a)(1), this word count does not include a count of the words in a table of contents, a table of authorities, mandatory notices under §42.8, a certificate of service or word count, or appendix of exhibits or claim listing. Furthermore, in accordance with 37 C.F.R. §42.24(d), this word count is the word count of the word-processing system used to prepare the paper.

Date: April 4, 2025

/ David R. Jaglowski /
David R. Jaglowski
Registration No. 58,514
THOMPSON HINE LLP
41 South High Street, Suite 1700
Columbus, Ohio 43215

CERTIFICATE OF SERVICE

Pursuant to 37 C.F.R. §§42.6 and 42.105, the undersigned hereby certifies that a true and correct copy of the Petition for *Inter Partes* Review in connection with U.S. Patent No. 11,941,817 and supporting evidence was served on April 4, 2025, upon agreement of the parties, via electronic mail on the following counsel of record for Patent Owner, EXINI:

Ronan Adato
William R. Haulbrook
Stephanie L. Schonewald
CHOATE HALL & STEWART LLP
Two International Place
Boston, MA 02110
radato@choate.com
whaulbrook@choate.com
sschonewald@choate.com

Courtesy copies were also served via electronic mail on Patent Owner's counsel of record in a related district court litigation:

Michael H. Bunis
Anita M.C. Spieth
John C. Calhoun
CHOATE HALL & STEWART LLP
Two International Place
Boston, MA 02110
mbunis@choate.com
aspieth@choate.com
jcalhoun@choate.com

Date: April 4, 2025

/ David R. Jaglowski /
David R. Jaglowski
Registration No. 58,514

THOMPSON HINE LLP
41 South High Street, Suite 1700
Columbus, Ohio 43215